UNIVERSITA' DEGLI STUDI DI VERONA

DIPARTIMENTO DI PATOLOGIA E DIAGNOSTICA

SCUOLA DI DOTTORATO DI SCIENZE BIOMEDICHE TRASLAZIONALI

DOTTORATO DI RICERCA IN BIOLOGIA E PATOLOGIA MOLECOLARE E CELLULARE

CON IL CONTRIBUTO DELLA LEGA ITALIANA FIBROSI CISTICA

CICLO XXV

CYSTIC FIBROSIS TRANSMEMBRANE CONDUCTANCE REGULATOR (CFTR) IN HUMAN LEUKOCYTES

S.S.D.: MED04

Coordinatore: Prof. Marco A. Cassatella
Firma:

Tutor: Dott.ssa Paola Melotti
Firma:

Dottorando: Dott.ssa Genny Verzè
Firma:

INDEX 1

ABSTRACT

AIM: 1) to evaluate the cystic fibrosis transmembrane conductance regulator (CFTR) protein expression and functional activity in monocytes; 2) to create immortalized cell lines from human B-lymphocyte cells characterized by different genotypes; 3) to evaluate CFTR protein expression in immortalized B cells.

BACKGROUND: Cystic Fibrosis (CF), the most common autosomal severe disorder in Caucasians, is caused by mutations in the CFTR gene. Although CF is a multi-organ disease, the lung pathology is the main cause of morbidity and mortality of CF patients. It is characterized by chronic inflammation as a consequence of persistent bacterial infections by several opportunistic pathogens. Mechanisms leading to increased susceptibility to bacterial infections in CF are not completely known, although the involvement of CFTR in microbicidal functions of macrophages is emerging. Tissue macrophages differentiate in situ from infiltrating monocytes and display a remarkable variability in cell morphology although common molecular and cellular functions.

Although expression of CFTR in alveolar macrophages has been described, its expression has not been reported in monocytes that are more accessible for expression studies and functional analysis tests than macrophages.

Evaluation of expression and functional activity of CFTR in peripheral blood mononuclear cells (PBMC) is a pre-requisite to evaluate their role and their potential use in diagnostic and developing new drugs acting on the molecular defect of CF.

METHODS: Purification of monocytes and lymphocyte B cells from whole blood; production of Epstein-Barr Virus (EBV); immortalization of Lymphocytes B cells by EBV; RNA isolation and CFTR mRNA analysis by reverse-transcription and polymerase chain reaction (PCR); quantitative real-time PCR (RT-*q*PCR); western Blotting; Flow cytometry assay; immunofluorescence; cell depolarization assay; Nasal Potential Differences (NPDs) assay; analysis of cell depolarization assay data.

RESULTS: In this study western blotting using a polyclonal and two monoclonal anti-CFTR antibodies that recognize different epitopes detected all known forms of CFTR. Flow cytometry and confocal microscopy analysis confirmed expression of CFTR protein expression and its membrane localization.

Increased fluorescence intensity, corresponding to membrane depolarization, was observed only when non-CF monocytes were stimulated with CFTR agonist, while CF monocytes did not show fluorescence variation. These results suggested a correlation between CFTR activity and membrane depolarization and data were confirmed using a specific CFTR inhibitor, CFTR (inh)-172.

This approach was compared to NPD measurements performed in a subset of the same patients subjected to this analysis. Results obtained by NPD overlapped those obtained by the analysis of monocytes from non-CF donors and CF patients.

B-lymphocytes were then immortalized by EBV and were tested as potential cell models for CFTR activity assays.

The major glycosylated form of CFTR was detected in immortalized non-CF EVB-transformed B cell line by a monoclonal anti-CFTR antibody, but a band with minor molecular weight was also detected with this antibody and with a polyclonal anti-CFTR antibody. Flow cytometry and confocal assay allowed us to confirm CFTR expression and membrane location in these cell lines.

Membrane depolarization test was applied in EBV-transformed B cells and the results confirmed a stimulus induced membrane depolarization in non- CF cells.

CONCLUSION: We have demonstrated that CFTR proteins are expressed in human monocytes as a variant recognized by a specific antibody. Its molecular weight is consistent with a lower level of post-translational processing and its loss in patients carrying a homozygous non-sense mutation confirmed its presence in human monocytes.

Flow cytometry could be also a useful method to evaluate CFTR expression. We demonstrated that it can distinguish between non-CF and HTZ subjects and CF patients analyzing stained CD14/Rb-AF488 monocytes.

Single-cell membrane depolarization analysis confirmed that, upon stimulation with CFTR agonists, normal monocytes displayed a highly reproducible membrane depolarization activity consistent with the expression of functional CFTR. Single-cell depolarization assay could be performed within a few hours after blood collection. It is also easily repeatable with a minimal discomfort and risk for the patient and it could thus allow a time-course evaluation of effects of any particular therapy on CFTR expression or functional activity. A specific activity index was devised that appears capable to discriminate among CF and non-CF cells. Overlapping NPD data and functional activity data, we observed a perfect correspondence. Since NPD is a reference diagnostic test applied when a subject has borderline sweat test and at least one unidentified CFTR mutation, we might promote the evaluation of CFTR activity in monocytes by optical techniques as a useful tool to assess CFTR activity for basic and translational research, including drug development and diagnosis.

As primary cells are available in limited amounts, we have taken advantage of the observation that CFTR-associated Cl^- permeability has been demonstrated in lymphocytes. So, immortalized-B-cells could be useful as cellular model to study CFTR expression and activity. We observed a form of CFTR that likely represents a processed isoform possibly linked to specific calpain activity in lymphocyte cells as demonstrated in the literature.

Furthermore, the index obtained by single-cell fluorescence imaging discriminated between non-CF and CF groups as shown in monocytes.

All these results demonstrated that CFTR protein is expressed and is active in human lymphocytes and EBV-transformed B cells opening interesting perspectives in this field. Indeed, these cells can be exploited to evaluate the response of specific mutations to newly developed drugs acting directly or indirectly on the basic defect of CF.

AIMS OF THE STUDY

As no published data was available describing CFTR expression and function in human peripheral blood monocytes, we sought to confirm and extend these findings by evaluating the actual expression of CFTR in blood and epithelial cells.

In addition, we aim at developing a CFTR functional assay in leukocytes isolated from peripheral blood. As one of the most frequently utilized functional test used to diagnose CF in subjects having atypical clinical manifestations, controversial sweat test and genetic analysis is NPD. This assay requires patient's collaboration, selection of subjects based of several criteria and it is time consuming for patients other than requiring the presence of two operators involved in the measurements. For this reason, we searched for a new functional assay that is less invasive and easier to perform.

Beyond the macrophages, lymphocyte cell lines have been studied for years in CF. The expression of the cyclic adenosine monophosphate (cAMP)-regulated chloride (Cl^-) channel, similar to that described for airway epithelial, was detected in both T and B lymphocytes suggesting a potential role of these cells in the pathophysiology of CF [1].

Sometimes, it is difficult to obtain biological sample from subjects because of geographic location, difficult shipping, age, condition of patients and etc. For this reason, we chose to establish lymphoblastoid cell cultures having the major advantages that they do not senesce and that they can be grown virtually indefinitely. This kind of cell line is obtained by EBV immortalization of B lymphocyte cells [2] extracted from peripheral blood (from CF and non-CF subjects).

In the area of interest of CF, some findings used lymphoblastoid cells from CF patients to study, for example, alternative splicing patterns [3] and study the feature of plasma membrane [4] in CF.

Finally, we sought to evaluate whether these cells could represent a valuable model for studying CFTR functional activity for applications like diagnosis and evaluation of response to drug targeting CFTR defect.

INTRODUCTION

Cystic Fibrosis

CF is a heterogeneous recessive genetic disorder in population of northern European descent. Its incidence is 1 in every 2500 live births and carrier frequency is approximately 1 in 25, but varies from country to country and with ethnic background. Precisely, 1 in 3000 white Americans develop the disease, 1 in 4000-10000 Latin Americans and 1 in 15000-20000 African Americans [5]. On the other hand, in Africa and in Asia the disease is uncommon with a reported frequency of 1 in 350000 in Japan [6].

The disease involves multi-organs system such as sinuses, pancreas, lung, liver, intestine and the sex organ. Pulmonary involvement occurs in 90% of patients and end-stage lung disease is the principle cause of death.

Classic CF is characterized by chronic bacterial infection of the airways and sinuses, fat maldigestion due to pancreatic exocrine insufficiency, infertility in males due to obstructive azoospermia and elevated concentrations of Cl^- in sweat.

CF is caused by a mutation of a gene in the long arm of chromosome 7 (about 180000 base pairs) encoding the CFTR (1480 amino acids), which is expressed in many epithelial cells and blood cells. It is an anion channel whose opening is mediated by agonist-induced increase in cAMP, followed by activation of protein kinase A (PKA), which phosphorylate channel proteins [7].

CFTR functions mainly as a Cl^- channel but it has many other regulatory roles including inhibition of sodium (Na^+) transport through the epithelial Na^+ channel (ENaC), regulation of the outwardly rectifying Cl^- channel, regulation of adenosine-5'-triphosphate (ATP) channels, regulation of intracellular vesicle transport, acidification of intracellular organelles and inhibition of endogenous calcium (Ca^+)-activated Cl^- channels [8] [9]. Furthermore, it is involved in bicarbonate (HCO_3^-)-Cl^- exchanges and a deficiency in HCO_3^- secreation leads to poor solubility and aggregation of luminal mucins [10].

The impact of defective Cl^- transport differs in various tissues. In epithelial cells of non-CF subject, the balance of Cl^- secretion through CFTR and Na^+ reabsorption through ENaC maintains a normal volume of airway surface liquid. On the other hand, absence or dysfunction of CFTR channels alters Cl^- secretion and Na^+ is hyperabsorbed. The net impact is an alteration of the salt and fluid balance that contributes to the dehydration of the airway surface liquid. Moreover, mucus builds up and clearance is decreased.

As in epithelial cells, in biliary and pancreatic ducts Cl^- channel defects result in loss or reduction of Cl^- secretion. On the opposite, in the sweat gland Cl^- ions are normally reabsorbed through CFTR channels to regulate sweat electrolyte levels. So, CFTR dysfunction leads to a loss of Cl^- ion reabsorption resulting in a high level of Cl^- in the sweat emerged on the skin. This is the reason why sweat Cl^- can be used as a biomarker to diagnose CF disease.

Active Na^+ absorption is also increased in CF airway and these concomitant ionic changes increase water reabsorption from the lumen.

Well over one thousand mutations have been described that can affect the CFTR gene and the vast majority of these are rare (The cystic Fibrosis Mutation Database. http://www.genet.sickkids.on.ca/cftr. Accessed March 20, 2009). These mutations are classified in six classes on basis of the mechanism by which they are believed to cause disease (fig.1) [11].

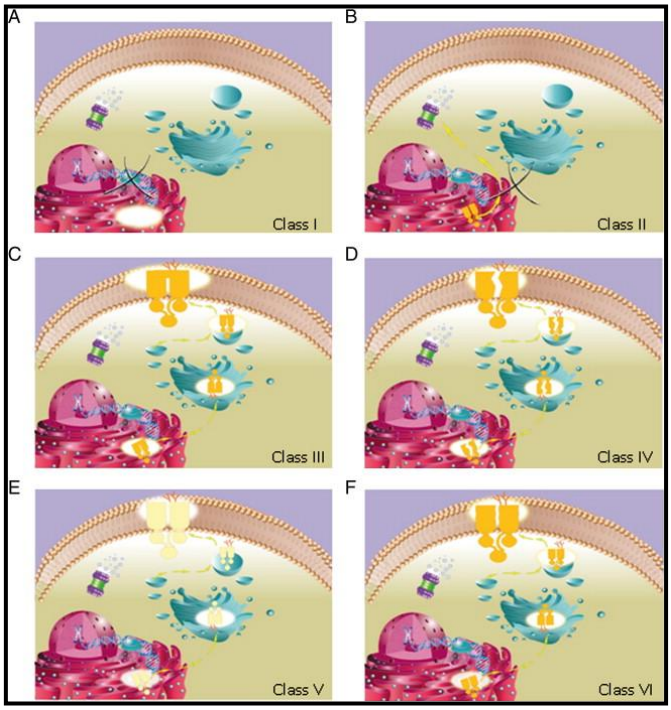

Fig.1. Categories of CFTR mutations. In classes I and II, a major fraction of the CFTR protein does not reach the apical epithelial cell surface. In classes III to VI the protein is expressed on the cellular surface but with altered or limited function: defective regulation in class III; defective conductance in class IV; partially defective production or processing in class V; functional and unstable CFTR at the apical membrane in class VI. Figure taken from Bob Lubamba et all. [12]

The most common CFTR mutation is a deletion of just three DNA nucleotides, which leads to the deletion of an amino acid (phenylalanine) at position 508 of the protein sequence. Denoted F508del, it is responsible for 70% of CF alleles and more than 90% of CF patients have at least one F508del allele. The defective protein retains substantial Cl^- channel function in cell-free lipid membranes. When synthesized by the normal cellular machinery, however, the protein is rapidly recognized as misfolded and is degraded shortly after synthesis, before it can reach its crucial site of action at the cell surface. Several other clinically important mutations, such as N1303K, G85E and G91R, lead to misfolded CFTR protein that is prematurely degraded. Approximately, 5% to 10% of CFTR mutations are due to premature truncations or nonsense alleles, such as G542X, R1162X.

Other CFTR mutations encode properly processed, full-length CFTR protein that lacks normal ion-channel activity. The G551D mutation (class III), for example, possesses little or no Cl^- channel function in vivo caused by an abnormal function of a nucleotide-binding domain. The A455E mutation (class IV) exhibits only partial CFTR ion-channel activity, a feature that probably explains a less severe pulmonary phenotype.

Other mutation classes include reduced numbers of CFTR transcript (class V) and defective CFTR stability at the cell surface (class VI).

The disease spectrum has broadened as it has become clear that there are a large number of CFTR mutations. Some conditions caused by two CFTR mutations might cause only mild lung disease with or without affecting the pancreas: these conditions can be described as “atypical CF.”

Other conditions do not meet the usual diagnostic criteria for classical CF and can be referred to as “CF-related disease,” for example congenital bilateral absence of the vas deferens, which can cause sterility in males.

Diagnosis of CF

Elevated sweat Cl^- concentration offers a convenient diagnostic test. The pilocarpine iontophoresis technique of Gibson and Cooke [13] rendered such testing practical: pilocarpine is introduced into the skin by iontophoresis where it produces localized sweating. The process of iontophoresis is almost completely painless and requires only 5 minutes. Rapid sweating continues for about 30 minutes after stimulation, long enough for an adequate collection to be made. Few tests in clinical medicine have the discriminating power of the “sweat test.” Nearly every patient with a clinical diagnosis of CF has an elevated sweat Cl^- concentration and only few other conditions, clinically quite distinct from CF, produce elevated sweat electrolytes.

After the sweat test came into general use, the diagnosis of CF was made on the basis of a sweat Cl^- concentration of 60 mEq/L or greater plus either a sibling or first cousin with CF, or lung disease of appropriate character, or pancreatic insufficiency. Since sweat concentration increases with age, sweat test must be interpreted in an age-specific fashion.

After 1989, when the CF gene was identified [14], the diagnosis could be made by molecular analysis of the CFTR gene. DNA-based testing for CF is useful when sweat test is not feasible or results are borderline or highly variable and it is performed in molecular genetic laboratories with CFTR mutation panel for the major racial and ethnic populations served.

Increasingly, patients are identified by newborn screening: immunoreactive trypsin levels (IRT), measured in blood spots collected at birth, are elevated in most patients with CF [15], but the cutoffs that capture nearly all patients with CF also capture five to six times that number of babies who do not have CF.

Although the elevated IRT levels seen in infancy in CF soon decrease, IRT levels in older CF patients appear to reflect quite closely the capability of that patient to secrete enzymes [15]. It can be helpful in separating CF patients whose ability to secrete enzymes is preserved from those with diminished exocrine pancreatic function.

Usually, screening for CF mutations or a second IRT test often follows IRT screening. Definitive diagnosis, however, still depends on either sweat testing or identification of two mutant alleles and one must take care not to dull the suspicion of CF in older children and even adults in the proper clinical setting, since screening will not identify all patients.

Most often, the clinical phenotypes of CF patients involve only one organ system, so that symptoms are limited to chronic bronchial infection, bronchiectasis, severe asthma, chronic sinusitis or chronic or recurrent pancreatitis. In these situations, extensive genetic studies often identify only one *CFTR* mutation or genetic variations with unclear pathogenic potential. In cases with such an equivocal diagnosis, testing CFTR function may help to reach a definitive CF diagnosis. CFTR-dependent Cl^- secretion is absent in classic CF disease, but is normal or minimally reduced among heterozygotes (HTZ). It can be indirectly assessed across the nasal epithelium by measuring changes in transepithelial NPD after pharmacologic activation of PKA.

This test, therefore, helps to diagnose patients with CF-like symptoms, to distinguish those with non-classic CF and to evidence CFTR dysfunction from those whose normal CFTR function indicates that they are unlikely to have CF.

NPD should be considered for assessing the risk of developing a clinical phenotype consistent with CF for patients with mutations that have a wide phenotypic spectrum or uncertain clinical relevance or when only one or even no mutation is found [16].

In questionable CF, mild or mono-symptomatic phenotypes frequently cause diagnostic difficulties despite detailed algorithms. CFTR-mediated ion transport can be studied ex vivo in rectal biopsies by intestinal current measurement (ICM).

The ICM technique allows the registration of CF-induced changes in electrogenic transepithelial ion transport (Cl^-, HCO_3^-, potassium (K^+)) in a Cl^- secretory epithelium, and on the basis of pharmacological criteria, is able to discriminate between CFTR-mediated Cl^- secretion and secretion through alternative anion channels [17]. ICM is an important tool for functional assessment in CFTR mutations of unknown clinical relevance and for confirmation of CF in the absence of two disease-causing CFTR mutations, exclusion of CF despite intermediate sweat test and age groups unsuitable for NPD measurements [18] [19].

Normal Biosynthesis of CFTR Protein: from Gene to Channel

The human CFTR gene encodes an integral membrane glycoprotein. Sequence analysis indicates that CFTR is a member of the “traffic ATPase” or ABC transporter superfamily and alignment with other members of this family suggests the existence of five distinct structural domains: two membrane-spanning domains (MSD), each composed of six membrane-spanning helices, two nucleotide-binding domains (NBD) and one central regulatory “R domain”.

Like other integral membrane glycoprotein, the initial stages of CFTR biogenesis begin with the formation in the endoplasmatic reticulum (ER) membrane of a core-glycosilated 135-to 140-kDa “immature” form, that is a precursor of the mature 160-to 180-kDa CFTR. The biogenesis (Fig.2) starts on cytosolic ribosomes that are targeted through the signal recognition particle (SRP) to the ER membrane translocon (Sec61 complex) via the SRP receptor [20].

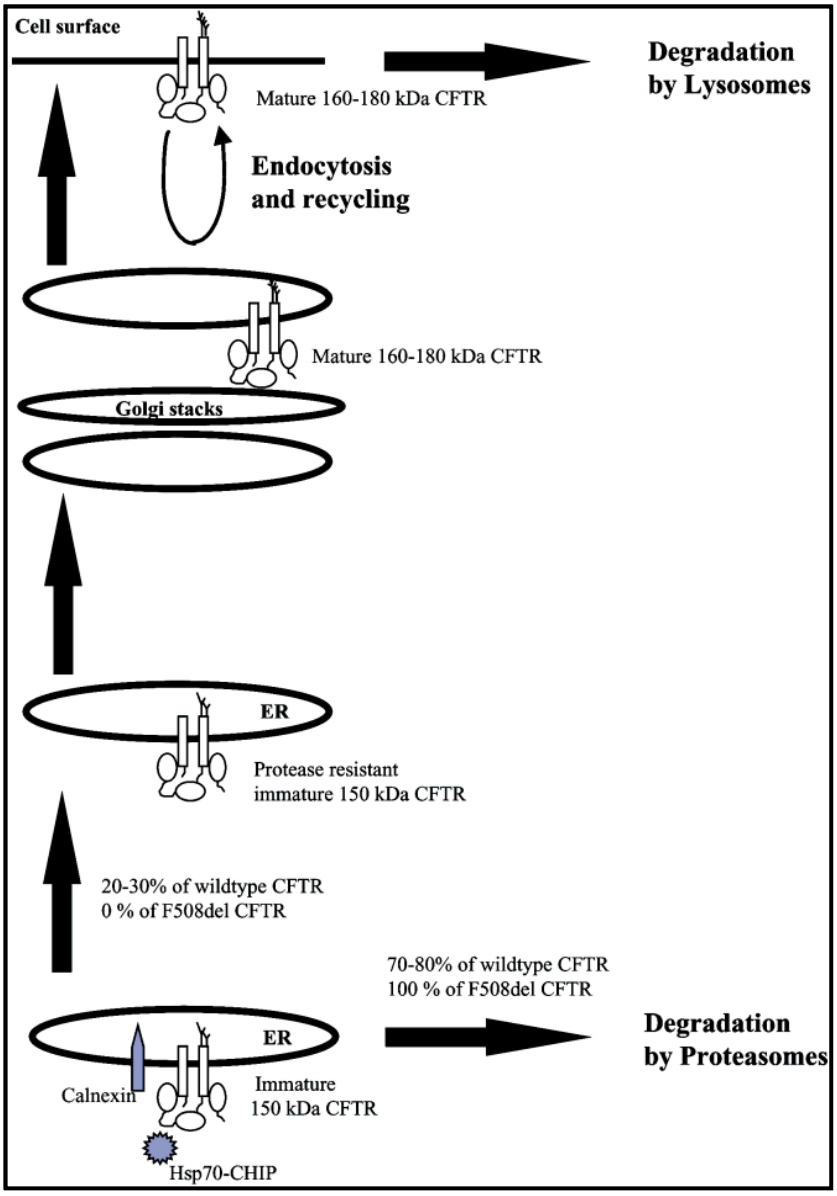

Fig. 2. **Maturation model of wild-type and F508del CFTR**. Both wild-type and F508del CFTR enter the endoplasmic reticulum during co-translational transport processes. Wild-type CFTR then folds, with the aid of chaperone molecules, such as calnexin and Hsp70-CHIP, into a protease resistant form that is able to leave the ER and will further mature in the Golgi-stacks before it reaches the cell surface. Once present at the cell membrane, the protein is recycled through cycles of endo- and exocytosis. The protein is ultimately degraded in lysosomes. The majority of wild-type translation products, and almost all F508del CFTR, is not able to fold into the protease resistant form in the ER and will be degraded by cytosolic proteasomes. Figure taken from Anne Vankeerberghen et all. [9]

The polypeptidic chain of CFTR emerging from the ribosome is thus co-translationally inserted into the ER membrane through the sequential and coordinated action of signal and stop transfer motifs. Additionally, CFTR may also follow an alternative mechanism of post-translational insertion into the ER membrane in

which one of the TM segments functions as the starting signal for translocation [20]. Normally, N-linked glycosyl groups are added to the polypeptidic chain of CFTR constituting the core-glycosylated form known as band B.

During the secretory pathway, the polypeptidic chain of CFTR undergoes different post-translational modifications at its glycan moiety to produce the fully glycosylated mature form known as band C (170-to 180-kDa). Several molecular chaperones assist the productive folding of CFTR nascent polypeptides in the cytoplasm: Hcs70/Hsp70 [21] assisted by the co-chaperones Hdj-2 and Hdj-1 [22] [23], Hsp90 [24] and calnexin (ER transmembrane lectin with chaperoning activity) [25]. The latter ER membrane chaperone transiently binds to the ER (immature) form of CFTR and appearance of the fully glycosylated mature form was shown to be concomitant with its dissociation. Similarly, complexes of F508del with Hsp70/Hsc70 were found to be more stable than those with wt-CFTR [21].

The mechanism underlying CFTR transport from the ER to the proteasome was shown to include Sec61β and a cytosolic, deglycosylated CFTR intermediary [26]. Distinct signals and recognition steps recruit a broad population of misfolded proteins to the ER associated degradation (ERAD) or glycoprotein ERAD (GERAD). They are the cellular disposal proteolytic machinery that uses the translocon for retrograde transport and ends up in the proteasome [27].

In the ER, substrates are either sorted for retention in the ER or are transported to the Golgi apparatus via coat protein II (COPII)- coated vesicles. Proteins transported to the Golgi are retrieved to the ER via the retrograde transport system. Ultimately, both retained and retrieved proteins converge to common machinery at the ER for degradation [28]. Furthermore, it was demonstrated that the gene *BST1* plays a novel role specific to the retrieval pathway required for the transport of misfolded proteins to the Golgi [28].

Both wt- and F508del-CFTR were found in pre-Golgi compartments but at lower concentrations than those found in ER. F508del-CFTR was never detected in post-Golgi compartments, but it was found in the ER-Golgi intermediate compartment (ERGIC) in CF cells [29]. The low level of CFTR in the Golgi region suggests a limiting step in selective recruitment of CFTR (even of wt) by the ER export machinery [30]. Therefore it seems that both retained and retrieved mechanisms serve to exert a quality control on CFTR in the early secretory compartments.

When CFTR reaches the apical membrane, it undergoes endocytosis and recycling. Clathrin-dependent endocytosis of CFTR relies on tyrosine-based and di-leucine-based motifs in the C-terminal tail of CFTR [31] [32].

Following internalization, CFTR recycles by default back to the cell surface with high efficiency. Recycling is absolutely necessary to maintain the long residence time of CFTR ($t_{1/2}$ of 14-18 hours) at the cell surface in the presence of constitutive internalization.

Regulation of CFTR channel gating and of CFTR function

CFTR has two NBDs, the site of ATP hydrolysis able to regulate channel gating. The two NBDs function as head-to-tail dimer with the ATP-binding sites located at the interface of the two subunits. Thus, the association of NBD1 and NBD2 is required for optimal adenosine triphosphatase (ATPase) activity by CFTR. Usually, NBD1 is a site of stable nucleotide interaction whereas NBD2 is a site of rapid nucleotide turnover. There is a model that describe CFTR channel gating (fig.3) [33] [9]

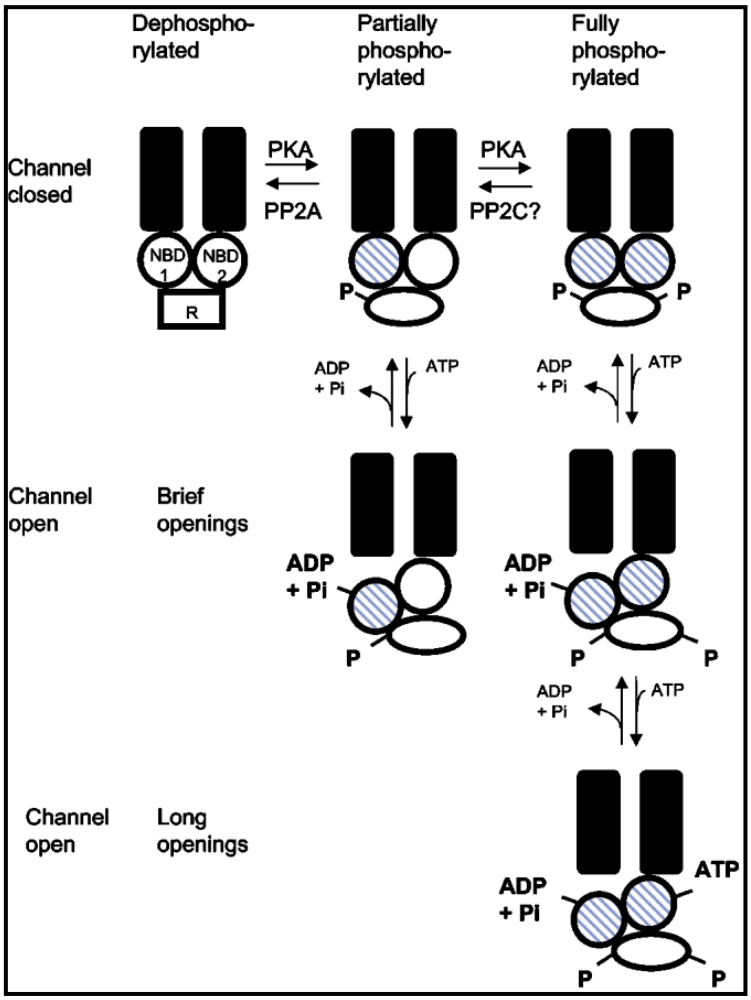

Fig 3. **Model of CFTR channel gating.** Activated NBDs are lined. Figure taken from Anne Vankeerberghen et all. [9]

Activation of the CFTR Cl^- channel starts with phosphorylation of the R domain by PKA. When CFTR is only partially phosphorylated, only the NBD1 is able to bind and hydrolyses ATP resulting in only brief openings of the Cl^- channel. On the other hand, when the R domain is fully phosphorylated, binding and hydrolysis of ATP by NBD1 results in opening of the channel and in binding of ATP at NBD2. So the anions can flow, according to the electrochemical gradient, through the pore formed by the transmembrane domains. In this way, a stabilization of the open state is achieved resulting in long openings of the channel. In a next step, when ATP is hydrolyzed at NBD2 and the hydrolysation products adenosine diphosphate (ADP) and pyrophosphate (P_i) are released at both NBDs, the channel closes. However, as long as the R domain is

phosphorylated, the cycles of binding and hydrolysis of ATP occur opening and closing of the channel continue. Once the R domain is dephosphorylated by phosphatases such as protein phosphatase 2A (PP2A) and 2C (PP2C), the channel closes and phosphorylation of the R domain by PKA is necessary in order to activate the channel again.

So, a crucial determinant of CFTR function is a phosphorylation of the R domain of CFTR. This domain contains multiple consensus phosphorylation sites of PKA and protein kinase (PKC). The R domain seems to function as an enzyme stimulating the interaction of ATP with the NBDs and multiple phosphoserines situated on the outside of an unstructured R domain interact with different sites on the NBDs to stimulate CFTR function [34].

Another model was proposed to understand the regulation of CFTR channel gating [35]. Indeed, It was demonstrated that CFTR has adenylate kinase activity harbored in NBD2 and that this activity regulates channel gating. In NBD2 both ATPase and adenylate kinase activities share an ATP binding site, but instead of releasing the γ-phosphate as in an ATPase, the adenylate kinase activity transfers the γ-phosphate to an AMP molecule. ATP binding to both NBDs influences CFTR gating, but in the presence of physiologic AMP concentration the predominant enzymatic reaction regulating channel activity is probably adenylate kinase [35]. Because the energy cost of adenylate kinase activity is very low compared to that of ATP, it was proposed that this activity and not ATP hydrolysis might control CFTR channel gating at physiological concentration of nucleotides.

Pathophysiology of CFTR

Chronic lung disease is the major cause of mortality and morbidity in CF patients. CF epithelia airway shows defective Cl^- secretion and increased Na^+ absorption due to mutations of the CFTR gene. These altered ion transport properties lead to defective antimicrobial activity of airway surface liquid (ASL) and dysregulation of ASL volume and deficient mucus clearance. As a result, CF mucus is more concentrated than mucus from healthy individuals indicating abnormalities of mucus hydration in CF patients. This consequence could be linked to activities of *CFTR* and *ENaC* genes. It is known that activation of wild-type CFTR led to inhibition of ENaC activity [36]. So, loss of CFTR regulatory function on ENaC results in increased Na^+ absorption in CF airway epithelia. Since the volume of ASL is determinate by the mass of salt on airway surfaces, increased ENaC activity and defective CFTR-mediated Cl^- secretion produce ASL volume depletion in CF airway epithelia. Normal airway epithelia have the capability to regulate the ASL volume by setting the height of the periciliary liquid (PCL), a layer that facilitates ciliary beating and cough clearance. In contrast, this PCL regulation fails in CF where it is reduced and cilia are collapsed onto cell surface, causing reduction of mucus transport rates.

ASL volume depletion constitutes the initiating events in the pathogenesis of CF lung disease (Fig. 4).

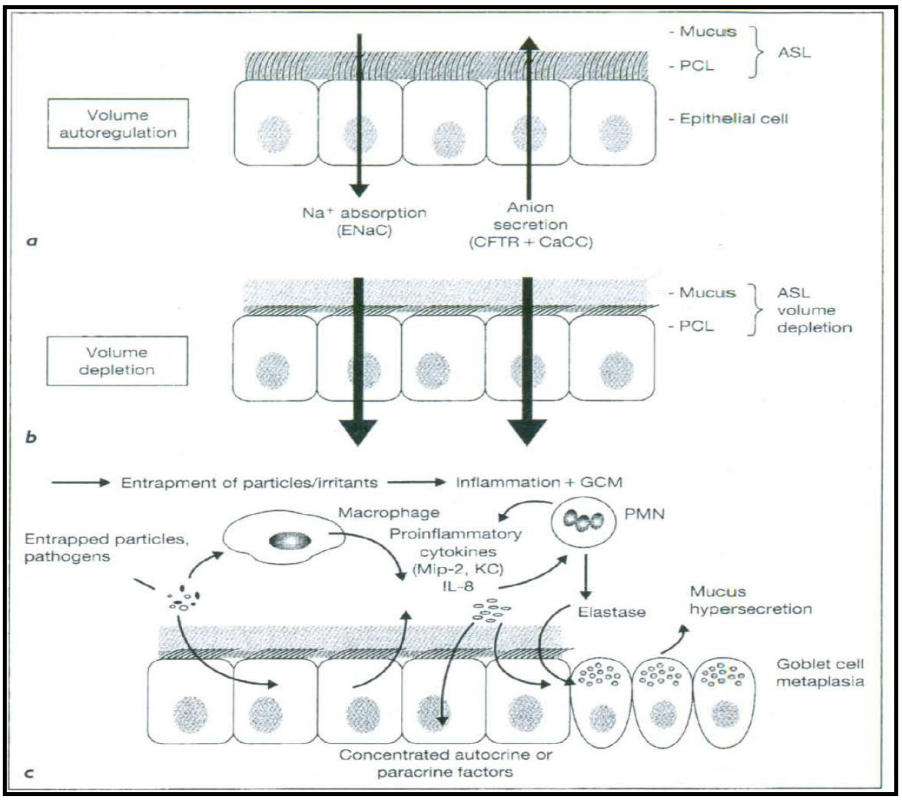

Fig.4. Schematic model of pathogenetic sequence of CF lung disease. Figure taken from Mall et all. [37]

In normal airways, a balance of ENaC-mediated Na^+ absorption and CFTR- and calcium-activated Cl^- channel (CaCC)-mediated Cl^- secretion adjusts ASL volume. Normal function of the mucociliary apparatus and efficient mucus clearance are certain. In CF airway, mucus is denser and PCL height is reduced resulting in attenuated mucus transport and clearance of inhaled pathogens. As a result, airway epithelia and macrophages release proinflammatory chemokines, like interleukin 8 (IL-8), which recruit neutrophils and trigger airway inflammation in the absence of bacterial infection. Neutrophils, in turn, release elastase that induces chemokines release by airway epithelia.

Infection and inflammation are critical in the progression of CF lung disease and are the cause of death of most patients. Bacterial infection could be a consequence of abnormality mucociliary clearance mechanism, but also of excess adhesion of bacteria to the CF airway and protracted inflammatory responses to prior viral infections. However, it is not yet clear if inflammation occurs prior to infection in the CF airway.

Certainly, after birth the lung of CF patients become infected by a variety of bacterial pathogens, such as *Pseudomonas aeruginosa*, *Burkholderia cepacia*, *Staphylococcus aureus* and *Haemophilus influenza*, with consequent neutrophilic infiltration recruited by elevated cytokine and chemokine production by already existing neutrophils and epithelial cells in the small airways.

Further, findings from lung lavage studies show that inflammation is present in children as young as 4 weeks of age who are apparently free of infection [38]. An increase in proinflammatory molecules such as

IL-8, interleukin 6 (IL-6), tumor necrosis factor alpha (TNF-α), and arachidonic acid metabolites has been found in patients with cystic fibrosis [39] [40].

Despite the high levels of cytokines, a significant decrease of interleukin 10 (IL-10) was found in CF [41] confirming the idea that regulation of the inflammatory function is aberrant.

Other cell types seem to have an important role in the inflammatory response in the airway. Neutrophils are clearly effector cells in the lung and their enzymes and oxidant products contribute to the ongoing damage in the airway. Neutrophils do not show altered function in CF compared to non-CF, but macrophages and lymphocytes have alterations in their function.

Excess inflammation in CF may be derived from aberrant activation of cell-signaling pathways. Nuclear factor-κB (NF-κB), required for transcription of many cytokines and chemokines, appears to be persistently activated [42] [43] due to continuous presence of reactive oxygen species (ROS) and lipopolysaccharide (LPS). Moreover, bacterial interaction with surface receptors on epithelial cells is a potent activator of NF-κB. The pro-inflammatory cascades are activated by interaction between cytokines released by macrophages and their receptors on epithelial cells. Normally, IL-10 inhibits NF-κB, but this process is down-regulated in CF. Also STAT-1 signaling is impaired in CF patients causing down-regulation of a variety of proteins such as nitric oxide synthase 2 (NOS2) [44] and interferon regulatory factor 1 (IRF1).

CFTR expression in leukocytes

Inflammation and infection as well as viscous secretions and impaired mucociliary clearance characterize the lung and airways of CF patients and contribute significantly to the morbidity and mortality associated with this disease. The epithelial goblet cells line the airway and are responsible for barrier function, secretions and mucociliary clearance.

However, the literature reveals that lung transplantation does not reduce the frequency or severity of *Pseudomonas aeruginosa* infection [45], suggesting that other cells types also must play a role and be compromised in CF.

The immune cells assist in the host response to environmental perturbations by neutralizing pathogens. Studies have focused predominantly on the contributory role of defective airway clearance and airway epithelial production of pro-inflammation proteins, but more recent data have indicated that other cell types, such as lymphocytes [46] [47] [1], neutrophils [48], macrophages [49] [50] and even dendritic cells (DCs) [51], are affected directly by the absence of CFTR function, impairing their ability to resolve infections and inflammation. Thus, the pathophysiology of the CF lung is not simply the result of defective epithelial cell function but a combined effect of airway epithelial cell dysfunction and inefficient immune cell management of the inflammatory response to infection [52].

Airway inflammation and recurrent pulmonary infections play a central role in the progression of CF lung disease. CF has been characterized by a perpetuating cycle of airway obstruction as a results of deficient CFTR, chronic bacterial infection and a robust inflammatory response [53].

Macrophages have created a lot of interesting in CF research since they play an essential part of the immune response by presenting antigen to lymphocytes and ingesting and killing invading organism such as *Pseudomonas aeruginosa*. They express CFTR and use it for different cellular functions such as acidification mechanisms [54].

Since macrophages are cells produced by the differentiation of peripheral blood mononuclear cells (PBMCs) in tissues, we focused our attention on monocytes circulating in the peripheral blood. Findings have described monocytes as immune effectors cells for defense against microbial pathogens and tumor surveillance and have demonstrated that human monocytes express Cl^- channels, which seem to be involved in chemotaxis and adhesion of human blood monocytes [55].

Furthermore, another study suggested that circulating monocytes from CF patients are ‘‘locked’’ in an endotoxin tolerance state, which results at least in part from a notable down-regulation of TREM-1 expression [56], which makes monocytes unable to respond properly to LPS challenge.

Macrophages and mast cells are present at higher levels in CF airways even during fetal development [57] and airway inflammation is already present in CF infants prior to establishment of chronic infection [58] [59]. In addition, young children with CF have an increased number of alveolar macrophages (AMs) and CC-chemokines even in the absence of pulmonary infection [60]. These observation support the previously hypothesis that intrinsic abnormalities in the innate immune system may contribute to the disease process and that CF lung pathology is due to intricate cross-talk between dysfunctional epithelial and immune cells.

AMs, DCs and neutrophils regulate the inflammatory response to infection through pathogen recognition with cell surface receptors, such as Toll-like receptors (TLRs) [61], resulting in cytokine production and cells recruitment. TLRs, such as TLR-4, are efficient ligands for Gram-negative bacteria recognition and activation of the host’s innate immune response and its dysfunction has been documented in CFTR-deficient epithelial cells [62] and macrophages [63]. Functional CFTR directly or indirectly affects compartmentalization of TLR4 which is necessary for well-controlled TRL4 signaling and degradation. TLR4 is critical for adequate inflammatory response to LPS and is essential for preventing injury to the host. In resting cells, TLR4 is located both in Golgi and at plasma membrane and it constantly cycles between the plasma membrane and the Golgi. After LPS engagement, different events drive receptor to the degradation pathway required for the resolution of the inflammatory response. CF macrophages have abnormal TLR4 subcellular localization and increased TLR4 plasma membrane expression compared to WT cells [63], but not more TLR4 mRNA or total TLR4 protein than WT cells. Therefore, trafficking regulation and vesicular sorting are likely responsible for the increased plasma membrane TLR4 protein levels. Indeed, after activation and

internalization, TLR4 is retained in early endosomes of CF macrophages [63] [64] causing a decrease TLR4 degradation.

The lack of functional CFTR in macrophages also has been associated with abnormal acidification of cell organelles [54], abnormal lipid metabolism [65] and alteration of transcription factors [66] that can contribute to the hyper-inflammatory phenotype. Furthermore, macrophages from CF patients are hyper-responsive to acute LPS exposure [63] demonstrating functional CFTR is necessary for controlling the innate immune response in macrophages and intrinsic defects of such early players in the innate immunity may directly influence the cascade of events leading to CF lung disease.

Professional phagocytes have specialized pathways that ensure efficient killing of pathogens in phagosomes. A common element in these pathways is organelles acidification that facilitates the optimal functioning of various degradative enzymes, particularly in phagosomes. Indeed, low pH is required in several organelles for diverse functions in many cell types, such as maturation of secretory products and their final secretion by the exocytotic pathway and dissociation and recycling in the endosomal pathway. The vesicular proton-ATPases, proton pumps that use cytoplasmic ATP to load H^+ into the organelle generation, generates primarily low organelles pH. It was demonstrated that the CFTR-mediated Cl^- secretion is important in lysosomal and phagosomal acidification [54] and that CFTR is also expressed on phagolysosomes of neutrophils [67, 68] where its dysfunction affects neutrophils chlorination of phagocytosed bacteria.

CFTR is involved in a number of processes integral to AMs function that are driven by vesicular acidification. The most common disease-causing mutations of CFTR, such as F508del and G551D, leads to a decreased killing of internalized bacteria, decreased in the phagocytic activity and down-regulation in acidification of an endosome/lysosome like compartment in resting cells and in the phagosomal compartment in phagocytosing cells [69].

In response to phagocytosis, macrophages produce and release ROS, including hydrogen peroxide and superoxide anion, by a multi-component nicotinamide adenine dinucleotide phosphate (NADPH)-oxidase assembled at the plasma membrane [70]. Normally, in lung AMs, *Pseudomonas aeruginosa* infection triggers the rapid formation of ceramide-enriched membrane platforms, which cluster and stimulate the activity of NADPH-oxidase, thereby resulting in a release of ROS [71]. Acid sphingomyelinase is the enzyme responsible of ceramide release from sphingomyelin, whereas acid ceramidase degrades ceramide to sphingosine [72]. The alkalinization of vesicles such as phagosomes and lysosomes results in an imbalance in the activities of these pH-sensitive vesicular enzymes in CF macrophages. Indeed, upon acute infection with *Pseudomonas aeruginosa*, CF macrophages fail to respond adequately by activating acid sphingomyelinase showing an inability to release ROS and to kill *Pseudomonas aeruginosa* [65].

Also lymphocyte cell lines express CFTR and these cells extracted from CF patients show defective cAMP-dependent Cl^- conductance.

The CFTR gene is transcribed in normal B and T lymphocytes at levels below those of epithelial tissues but this low level of CFTR transcription is apparently sufficient to confer cAMP regulation of Cl^- current in lymphocytes [73].

Furthermore, activation of CFTR Cl^- current by nitric oxide (NO) was detected in human T lymphocytes [74]. It was suggested that NO acts as a transducer molecule in interleukin 2 (IL-2)-induced T lymphocyte clones, activating soluble guanylate cyclase and producing cGMP and initiating downstream events including the activation of CFTR. Cl^- currents have been implicated in several T lymphocyte functions, including volume regulation, cytolysis by cytotoxic T cell and calcium (Ca^{2+}) influx associated with T cell activation. It is not clear what CFTR contributes to each of these functions, but two regulated second messenger pathways converged on CFTR suggests that CFTR may play a role in normal immune function and that the abnormality in regulation of the CFTR function by two second messenger pathways may cause immune abnormalities.

Interestingly, studies have shown that Th2 lymphocytic response is predominant in CF lungs [75], characterized by a specific IL-4 response and by high antibody production, and lack of CFTR in $CD3^+$ lymphocytes leads to aberrant adaptive immune response.

Although the exact role of lymphocytes in chronic inflammation and bacterial infection in CF lungs is not well understood. It appears that CFTR mutations are associated with an inability to clear bacteria despite the infiltration of inflammatory cells, in particular lymphocytes, into airway epithelial layer.

The interaction between CFTR in lymphocytes and E-cadherin in epithelial cells was demonstrated to enhance epithelial HCO_3^- secretion through NF-κB-mediated up-regulation of CA expression. Normally, HCO_3^- ion has enhances antimicrobial activity indirectly by increasing the susceptibility to antimicrobial defense peptides. Defective CFTR in lymphocytes may impair the lymphocyte-enhanced epithelial HCO_3^- secretion and thus bacterial killing capacity [76].

Macrophages, natural killer cells and Th1- and Th2-type lymphocytes produce IL-10, a major regulatory cytokine of inflammatory responses identified as an inhibitor of IFN-γ, T-cell activation and pro-inflammatory cytokine production [77]. Changes in IL-10 secretion may efficiently contribute to the inflammatory response in CF. Moreover; data might demonstrate that Il-10 plays an essential role in tolerance against *Aspergillus fumigatus* and *Pseudomonas aeruginosa* in the lung of CF patients [77].

It was demonstrated that in non-CF lymphocytes the production of IL-10 increases when glutamate secretion is released by neutrophils in airway inflammation [78], while CF-lymphocytes were insensitive to glutamate. This event was explained by participation of mGluR1 in the enhancement of IL-10 secretion in normal lymphocytes. Indeed, IL-2 activated lymphocytes expressed mGluR1a/b on cell surface in association with CFTR through intermediary PDZ-containing scaffolding proteins. In contrast, T-cells derived from CF patients, are unable to express supramolecular complex containing CFTR and mGluR1a/b. Therefore, it could be supposed that reduced expression of mGluR1 in CF patients evokes at loss of sensitivity to glutamate in lymphocytes, which decreases the secretion of IL-10 and causes inappropriate

immune response to antigen [78]. The explanations for the reduction of mGluR1 in plasma membranes of CF-lymphocytes was not completely clear, but it seemed that competition for CFTR-associated protein (CAL) between CFTR and mGluR1a/b in CF lymphocytes down-regulate the trafficking of mGluR1a/b which occur in normal cells after T-cell activation. Thus, it is possible to conclude that CAL limits scaffolding and trafficking of mGluR1a/b in CF lymphocytes, where its overexpression in CF directs CFTR for degradation.

Functional studies in lymphocytes confirmed CFTR-mediated Cl^- conductance during the G_1 phase of the cell cycle and changes in inflammatory responses have been reported in CF lymphocytes, like reduced IFN-γ secretion by CD4+ T lymphocytes [79].

Th17 lymphocytes are also present in the submucosa of children with CF from early course of the disease [80] and could be the earliest drivers of the inflammatory response. The hypothesis is that early inflammation may be Th17 driven and subsequently a vicious cycle could occur in which the initial production of IL-17.

METHODS AND MATERIALS

Subjects

Healthy volunteers including obligate heterozygotes and individual undergone genetic analysis for CFTR mutations for genetic counseling purposes were recruited for the study. Samples and data were used for analysis only after that informed consent was obtained according to the guidelines approved by the local Ethical Committee. All clinical data were collected in the electronic database of the CF Center of Verona.

Purification of monocytes from whole blood

Monocytes were obtained from 5 mL of whole blood supplemented with 1 mM EDTA and isolated using the RosetteSep Human Monocytes Enrichment Cocktail (cat.# 15068 StemCell Tecnologies) at 50 μL/mL of whole blood. This cocktail contains a combination of mouse and rat monoclonal antibodies directed against cell surface antigens on human hematopoietic cells and glycophorin A on red blood cells.

After incubation with the Cocktail for 20 minutes at room temperature (r.t.), whole blood was diluted with an equal volume of Phosphate Buffered Saline(PBS) 1X (cat.#AM9625 Life Technologies) + 2% (v/v) fetal bovine serum (FBS) (Cambrex Bio Science) and 1 mM EDTA and layered on Ficoll-Paque^{TM} PLUS (cat.# 17144002 Ge-Healthcare Life Science). Centrifugation was performed at 1200 x *g* for 20 minutes with brake off. After centrifugation, enriched cells were removed from plasma interface of Ficoll-Paque^{TM} PLUS and washed with PBS 1X+2%FBS+1mM EDTA.

Platelets were removed using CD61 MicroBeads (cat.# 130-051-101 Miltenyi Biotec). Enriched cells were re-suspended in 80 μL of PBS 1X+0.5% FBS+2 mM EDTA per 10^7 total cells and 20 μL of CD61 MicroBeads was added for 10^7 total cells. After incubation at 4-8°C for 15 minutes, cells were washed and separated with MS column using a magnetic system. Unlabelled cells that passed through the column were collected.

Purification of B lymphocyte

Lymphocytes were obtained from 5 mL of whole blood supplemented with 1 mM EDTA. Whole blood was directly layered on Ficoll-Paque^{TM} PLUS and centrifuged at 400 g for 30 minutes. PBMCs were removed from plasma interface of Ficoll-Paque^{TM} PLUS and B cells were enriched using Human B Cell Enrichment Kit (cat.#19054 EasySep^{TM}) containing EasySep^{TM} Human B Cell Enrichment Cocktail and EasySep^{TM} D Magnetic Particles. The former contains a combination of monoclonal antibodies directed against surface antigens on human blood cells and dextran. The latter contains a suspension of magnetic dextran ion particles in TRIS Buffer.

PBMCs were re-suspended at a concentration of $5x10^7$ cells/ml in PBS+2% FBS+1 mM EDTA and incubated with EasySep^{TM} Human B Cell Enrichment Cocktail at 50 μL/mL cells for 10 minutes at r.t.. After this period, EasySep^{TM} D Magnetic Particles were added at 75 μL/mL cells for 5 minutes at r.t.. The cell suspension was

brought up to a total volume of 2.5 ml by adding PBS+2% FBS+1 mM EDTA and the tube was placed into a magnet.

After 5 minutes, the desired fraction was poured off into a new tube, while magnetically labeled unwanted cells remained bound inside the original tube.

Cell cultures

16HBE14o$^-$ cell line [81], with non-CF phenotype immortalized human bronchial epithelial cell expressing endogenous WT CFTR, (kind gift from Pamela Davis, Case Western Reserve University School of Medicine, Cleveland, OH, USA) were grown in Earle's MEM (cat.#B4800 Cambrex Bio Science) supplemented with 10% FBS and 1% L-glutamine (Cambrex Bio Science).

IB3 cell line [82], immortalized bronchial epithelial cells derived from a CF patient carrying W1282X and F508del mutations (a kind gift from Pamela Zeitlin, Johns Hopkins University, Baltimore, MD, USA) was grown in LHC-8 medium without gentamicin (cat.#12678-017 Invitrogen) supplemented with 5% FBS.

Suit-2 cell line [83], pancreatic cell line derived from a liver metastasis of human pancreatic adenocarcinoma, CFPAC [84], with CF phenotype (pancreatic adenocarcinoma cell line homozygous for the F508del mutation) and B95.8 cell line, EBV-transformed marmoset blood leukocytes were grown in RPMI 1640 (cat.#R0883 Sigma-Aldrich) supplemented with 10% FBS and 2mM L-glutamine.

Cell lines were cultured at 37°C in a humidified atmosphere with 5% CO_2.

Production of EBV

B95.8 cell line were grown and expanded in flask. When desired volume was reached, maintenance of the cells was stopped and after 10 days the cells were centrifuged at 1400 x g for 15 minutes. The supernatant containing EBV was filtered through a sterile 0.45 μm filter and then through a sterile 0.22 μm filter.

Immortalization of Lymphocytes B cells by EBV

Lymphocyte B cells obtained from subjects were washed twice with RPMI 1640 without FBS. The supernatant containing EBV was added to cell pellet in a polypropylene tube and incubation was done at 37°C in a humidified atmosphere with 5% CO_2 for not more than 18 hours. The tube was maintained partially open. After that period, EBV-transformed B cells were washed with RPMI1640 without FBS and then re-suspended in RPMI1640 supplemented with 10% FBS and 2mM L-glutamine and placed into a 48-wells cell culture plate.

Immortalized cell lines were cultured at 37°C in a humidified atmosphere with 5% CO_2.

RNA isolation and CFTR mRNA analysis by reverse-transcription and polymerase chain reaction (PCR)

Monocytes were homogenized with Trizol^{R} Reagent (cat.# AM7020 Life Technologies) for 5 minutes with a volume of 1ml reagent for 5-10 x 10^{6} cells. Then, 200 μl chloroform per 1 ml Trizol^{R} Reagent was used and the tube was shaken vigorously for 15 minutes. After centrifugation at 12000 x *g* for 15 minutes at 4°C, the aqueous phase was removed and 500 μl 100% isopropanol per 1 ml Trizol^{R} Reagent was added. After incubation for 10 minutes and centrifugation at 12000 x *g* for 10 minutes at 4°C, RNA was washed with 75% Ethanol and re-suspended in RNase-free water. 1 μg of total RNA was reverse transcribed in a volume of 20 μl using 1 μM random primer (cat.#48190-011 Invitrogen) and 200 U SuperScriptII (cat.#18064-014 Invitrogen) at 42°C for 1 hour. PCR was performed in a GeneAmp PCR System 9700 (PE Applied Biosystem, Milan) for 35 cycles (30 second denaturation at 94°C, 30 second annealing at 60°C and 50 second elongation at 72°C) in a volume of 25 μl reaction buffer containing 0.75 U AmpliTaq (cat.#4311806 PE Applied Biosystem), 400 μM of each primer, 200 μM dNTP (cat.#11581295001 Roche, Milan). Primers used were: ACTB 170F 5'-ATCAAGATCATTGCTCCTCCTG-3'; ACTB 170R 5'-GCAACTAAGTCATAGTCCGCC-3'; CFTR 771F 5'-GGGGAAGTCACCAAAGCAGTACAGC-3'; CFTR771R 5'-GCGCAGAACAATGCAGAATGAGATGG-3. These *CFTR* primers give a predicted product of 771 bp that was used as a template for the following PCR, which was performed as above with the following primers (CFTR 338F 5'-TCACATTGGAATGCAGATGAG-3'; CFTR 338R 5'-GTCTTTCACTGATCTTCCCA-3') expected to amplify a 338 bp product when exon 5 is present in the cDNA and of 248 bp if the exon 5 is skipped. Actin mRNA amplification was performed for 22 cycles on the cDNA as positive control of reaction efficiency.

Quantitative real-time PCR (RT-*q*PCR)

Total RNA was extracted from 16HBE, IB3-1, lymphoblastoid cells derived from non-CF subjects and CF patients with different genotype with High Pure RNA Isolation Kit (cat.#11828665001 Roche, Milan) according to manufacturer's instructions. cDNA synthesis was achieved using High-capacity cDNA Reverse Transcription kit (Applied Biosystem) using 1 μg of total RNA in a volume of 20 μl containing 1 μM random primer (cat.#48190-011 Invitrogen) and 200 U SuperScriptII (cat.#18064-014 Invitrogen). The Reverse-transcription PCR was performed at 42°C for 1 hour. RT-*q*PCR was performed using Platinum SYBR Green qPCR SuperMix-UDG (cat.#11733-038 Invitrogen) in a StepOne (Applied Biosystem) detection system under the following conditions: 2 min at 50°C, 2 min at 95°C, 40 cycles of 95°C for 15 s, 60°C for 30 s. CFTR transcripts with a nonsense mutation were quantified by primers that recognized only non-F508del transcripts [85] (forward primer 5'-GCACCATTAAAGAAAATATCATCTT-3', reverse primer 5'-TTGTCTTTCTCTGCAAACTTGG-3'). Glyceraldehyde-3-phosphate dehydrogenase (GAPDH) was used as

housekeeping gene (forward primer 5'-GAAATCCCATCACCATCTTCCAGG-3', reverse primer 5'-GAGCCCCAGCCTTCTCCATG-3'). Relative quantification was performed using the $\Delta\Delta C_t$ method [86].

Western Blotting

Monocytes and epithelial cell lines were lysed with a Lysis Buffer containing 1% Triton X-100, 50 mM Tris (pH 7.4), 150 mM NaCl, 200 μM $NaVO_4$, 1mM DTT, 10 mM NaF, 1mM EDTA and protease inhibitor cocktail (cat.#05892791001 Roche). Proteins were quantified by Bradford methods and about $20\mu g$ of protein for each samples were denatured in Laemmli sample buffer for 20 minutes at 40°C or 10 minutes at 95°C. The separation was performed in SDS gel containing 6% acrylamide and transferred onto nitrocellulose membrane (Millipore Corp, Bedford, MA). Membranes with transferred proteins were incubated over night at 4°C with 0.3 μg/ml polyclonal anti-CFTR (cat.#ACL-006 Alomone Labs) or 0.5 μg/ml of either of the two monoclonal anti-CFTR antibodies clones 13-1 and 24-1 (cat.#MAB1660 and #MAB25031 respectively R&D Systems). In all cases detection of the primary antibody was performed with HRP conjugated secondary antibody (cat.#NA931-1ML GE Healthcare) followed by ECL detection (cat.#21246 Millipore).

EBV-transformed B cells were immunoprecipitated using ACL-006 as anti-CFTR antibody. Protein extracts were added to anti-CFTR antibody and incubated at 4°C for 3 hours. After washing, Protein G-Sepharose 4 Fast flow conjugate (cat.#17-0618-01 GE Health care) was added to protein-antibody complex and incubated for 1 hours at 4°C. The complexes were washed three times and then denatured in Laemmli sample buffer for 20 minutes at 40°C. The protein separation and western blotting were set with the same method used for monocytes with some changes. Indeed, the protein separation was performed in SDS gel gradient 6-12% acrylamide and membranes were incubated overnight at 4°C with or 0.4 μg/ml polyclonal anti-CFTR (ACL-006) or with 0.5 μg/ml monoclonal anti-CFTR antibody clone CF3 (cat.#ab2784 Abcam^R).

Flow cytometry assay

Some μl (about 100) of peripheral blood withdrawn into vacutainer® EDTA tubes was used for flow-cytometry assay. Red blood cells were lysed by adding 1 mL solution containing 0.89% NH_4Cl, 0.10% $KHCO_3$ and 0.2 mM EDTA. Lysis was stopped by adding PBS containing 5% FBS and then centrifuged at 300x*g* at r.t.. After discarding supernatant, 10 μl human serum (HS) (cat.#H4522 Sigma-Aldrich) was added to the remaining supernatant and then an anti-CD14 antibody conjugated with PE-Cy7 fluorochromes was added and incubated for 30 minutes. Cells were washed with PBS containing 5% FBS and centrifugated. After removing supernatant, cells were fixed 20 minutes at room temperature by adding 0.5 mL Fixation buffer (cat.#420801 BioLegend). After being centrifuged, cells were washed once with PBS 1X and twice with Permeabilization Wash Buffer (PWB) (cat.#421002 BioLegend) to permeabilize cell membranes. HS was added and monocytes were incubated with 10 minutes before adding 0.8 μg or 0.15 μg (lot n. AN-04 and

AN-05 respectively) polyclonal anti-CFTR antibody ACL-006 or adding the same quantity of anti-CFTR antibody pre-incubated one hour at +4°C with 4 μg/sample blocking peptide corresponding to aminoacids 1468-1480 of CFTR. After 45 minutes incubation at r.t., cells were washed twice and incubated 25 minutes at r.t. with 1.5 μg Goat anti-Rabbit IgG/AF 488 (cat.#A-11008 Invitrogen). Cells were washed twice as above and analysed at MACSQuant Analyzer (Miltenyi Biotech, Cologne, Germany) using 488 nm for excitation. No compensation was needed for the used fluorochromes. A total of 80.000 events, containing 1000-3000 monocytes, were registered and Flow Cytometry Standard files (FCS-files) were analyzed with FCS Express v3 software (De Novo Software, Los Angeles, U.S.A.). For statistic analysis of data, Prism4 software (GraphPad Software Inc., La Jolla, U.S.A.) was used. A Gaussian distribution of all values from each group was confirmed and a one-way ANOVA was used to compare means of variables between groups, followed by Bonferroni's multiple comparison post-hoc test to compare all means. Statistical significance was accepted at $p \leq 0.05$.

EBV-transformed B cells were also analyzed by flow cytometry assay. Cells were washed twice with PBS 1X, re-suspended in 100μl of PBS1X and incubated with 10% Goat Serum (GS) (cat.#H4522 Sigma-Aldrich) for 15 minutes. After incubation, some cells were incubated with 48,7 μg monoclonal antibody anti- CFTR clone CF3 (cat.#2784 Abcam) and some cells with the same quantity of Mouse IgM Isotype Control purified as negative control (cat.#14-4752-81 eBioscience). After 30 minutes at 4°C, cells were washed twice with PBS1X, re-suspended in 100 μl PBS1X and incubated with 1.5 μg Goat anti-Mouse IgM antibody conjugated with Alexa Fluor (AF) 488 (cat.#A21042 Invitrogen). After 30 minutes at 4°C, cells were washed once with Hank's Balanced Salt Solution (HBSS) 1X and re-suspended in 150μL HBSS supplemented with Vybrant® DyeCycle™ stain working solution 1000X (cat.#V35003 Life Technologies) for DNA content analysis in living cells. After 20 minutes of incubation, cells were analysed at MACSQuant Analyzer using 488 nm and 369 nm for excitation. No compensation was needed for the used fluorochromes. A total of 30.000 events of living cells were registered and Flow Cytometry Standard files (FCS-files) were analyzed with FlowJo software.

Immunofluorescence

Purified monocytes were seeded onto coverslips at a density of 450 cell/mm^2, let to adhere one hour and fixed 10 minutes with 4% paraformaldehyde in PBS (cat.#554655 BioLegend). After blocking and permeabilization respectively with 10% HS and 0.1% Triton X-100 (cat.#T8532 Sigma-Aldrich), cells were incubated with 1 μg/ml monoclonal anti-CFTR antibody clone 13-1 and then with 2 μg/ml Goat anti-Mouse IgG/AF594 (cat.#A11005 Invitrogen). Nuclei were stained with 3 μM DAPI (cat.#D9542 Sigma-Aldrich) and coverslips were mounted onto microscope sildes using less than 10 μl Anti-fade mounting medium. Coverslips were sealed with clear nail polish, let to dry and salt crystals were removed with water. Microscope slides were analysed at Leica TCS-SP5 confocal microscope (Leica Microsystem, Wetzlar, Germany).

EBV-transformed B cells were washed with PBS1X, re-suspended and incubated 15 minutes at 4°C with 10% GS. After that period, some cells were incubated with 18,25 μg/ml of Monoclonal antibody anti-CFTR clone CF3 and some cells were incubated without antibody as negative control. After 30 minutes of incubation at 4°C, cells were washed with PBS 1X and incubated for 30 minute at 4°C with2 μg/ml anti-Mouse IgM/AF488. Cells were washed and incubated 20 minutes at 4°Cwith 1 μg/ml Cell Mask Orange (cat.#C10045 Invitrogen) as plasma membrane stain. After two washes, cells were fixed with 0.5 mL Fixation buffer and, after 20 minutes of incubation at r.t., washed twice with PBS1X. Cells were incubated with 2 μM TO-PRO 3 (cat.#T3605 Invitrogen) as nuclear counterstaining. After 30 minutes of incubation at r.t., cells were washed with PBS1X, re-suspended in PBS 1X and let to adhere onto coverslip pre-treated with poly-L-Lysine for 1 hour at 37°C. After that period, coverslips were mounted onto microscope silde using less than 10 μl Anti-fade mounting medium and sealed with clear nail polish. They were then to dry and salt crystals were removed with water. Microscope slides were analysed at Leica TCS-SP5 confocal microscope (Leica Microsystem, Wetzlar, Germany).

Cell depolarization assay

CF and non-CF pancreatic adenocarcinoma cell lines (CFPAC and Suit-2 respectively), monocytes from non-CF, HTZ and CF patients and EBV-transformed B cells from non-CF and CF patients were used as model to monitor CFTR-dependent membrane potential (Vm) changes. The technique was performed using bis-(1,3-diethylthiobarbituric acid) trimethine oxonol ($DiSBAC_2(3)$) (cat.#1021 Invitrogen) as membrane potential-sensitive probe. It can enter depolarized cells where it binds to intracellular proteins or membrane upon which exhibits enhanced fluorescence and a red spectral shift. Increased depolarization results in additional influx of the anionic dye and an increase in fluorescence. Conversely, hyperpolarization is indicated by a decrease in fluorescence. It has excitation maxima of 530 nm and emission maxima of 560 nm. The method using this probe has already been described in detail [87]. Unlike CFPAC and Suit-2, before the assay monocytes were sedimented ($2x10^5$ cells/ml) onto a tissue culture dish (cat.#353001 Falcon) for 1 hour in RPMI1640 medium supplemented with 1 mM L-glutamine at 37°C and EBV-transformed B cells were sedimented (at $4x10^5$ cells/ml) onto a tissue culture dish coated with Poly-L-Lysine (cat.#P8920 Sigma-Aldrich) for 1hour in PBS1X. After 1 hour, RPMI1640 supplemented with 1 mM L-glutamine and 10% FBS was added to all plates and monocytes were kept at 37°C for 24 hours, while EBV-transformed B cells were analyzed 4 hours after preparation. At the time of assay, the cells were washed twice with a Cl^--free solution containing Na-gluconate 0.1 M, K-Gluconate 5μM, Ca-Acetate xH_2O 2 μM, Mg-Acetate $x4H_2O$ 2 μM, D-Mannitol 50 μM, D-Glucose 50 μM, HEPES-Na 5 μM. Cells were then perfused for 10 minutes at room temperature with Cl^- free solution containing 100 mM $DiSBAC_2(3)$. A baseline was acquired for 5 minutes before addition of a CFTR stimulus, consisting of a cocktail containing 500 μM 8-Br-cAMP (cat.#B5386 Sigma-Aldrich), 10μM Forskolin (cat.#F6886 Sigma-Aldrich) and 100μM 3-Isobutyl-1-

methylxanthine (cat.#I7018 Sigma-Aldrich). The recording was kept for 25 minutes after addition of stimulus. To evaluate the correlation between CFTR activity and membrane depolarization, the CFTR (inh)-172 (cat.#C2992 Sigma-Aldrich) was used at a final concentration of 10μM. In some experiments amiloride (cat.#A7410 Sigma-Aldrich) was added to a final concentration of 200μM to block epithelial Na^+ channels. The fluorescent signal was acquired on Zeiss microscope Olympus BXS1WI using a CCD intensified videocamera (Retiga EXi, Q-Imaging, Canada) and the software QED in vivo (MediaCybemetics, USA) at a rate of 1 frame/minute. $DiSBAC_2(3)$ was excited with a 100-watt mercury-arc lamp and 535/40 excitation and 630/30 emission filters. Data were presented as percentage of signal variation (ΔF) in relation to the time of addition of the stimulus, according to the equation: $\Delta F_t = [(F_t-F_0)/F_0]x100$, where F_t and F_0 are the fluorescence values in the absence of extracellular Cl^- ions at time t and at the time of addition of the stimulus respectively.

Nasal Potential Differences assay

Transepithelial NPD was determined by measuring the PD between a 1% agar-filled exploring bridge on the nasal mucosa and a reference bridge inserted into the subcutaneous space of the forearm. The exploring bridge is a double lumen catheter, with one lumen filled with Ringer's solution, while the reference bridge is a 21-g needle filled with Ringer's solution in 4% agar. The exploring bridge is also marked at 0.5 cm intervals. Ag^+/AgCl electrodes connected to a high-impedance voltmeter linked both bridges. Using direct vision with an otoscope, the exploring bridge was advanced through the inferior turbinate of both nostrils and PD was recorded at various sites. The probe was stabilized at most negative voltage and positioned with tape on the nose and forehead. The subject should sit relaxed and comfortably in an armchair so that the nasal perfusate flushed from the nostril without any discomfort. When the exploring bridge was placed, the perfusion of five solutions was started and for each solution NPD was measured for a minimum of 3 minutes obtaining a period of stable signal for at least 30 seconds. Baseline PD was determined by perfusion with Ringers and the responses to amiloride ($1x10^{-4}$M), Cl^- free (0 Cl^-), isoproterenol ($1x10^{-5}$M) and ATP ($1x10^{-4}$M) were sequentially registered.

The perfused solution should be warmed so that the temperature exiting from the exploring catheter was in the range from 32 and 37°C in order to obtain a larger activated chloride conductance. For that reason, the polyethylene tubing was passed through a water-jacketed tube proximal to the nasal probe. The software PowerLab (ADInstruments, UK) was utilized for acquisition and analysis of data. The data acquisition system ML870 PowerLab 8/30 was utilized in connection with the voltmeter Iso Millivolt Meter (World Precision Instruments, Sarasota (WPI), FI, USA). It was connected to Ag^+/AgCl electrodes MEH3S (World Precision Instruments, FI, USA) linked to the catheters. Smokers and subjects with nasal polyps or abnormal mucosa were not subjected to this test.

Analysis of cell depolarization assay data

Intensity of fluorescence recorded was transformed to % variation between time t and time 0 based on the followed formula: $\Delta F_t = [(F_t - F_0)/F_0] \times 100$. The first 5 time points were not considered from the analysis because of the perturbation caused by the addition of compounds and the time required for the system to reach equilibrium before starting the recording. Over this 5 minutes, the % variation and 3 phenotypic groups (CF, non-CF and HTZ) and their interaction were fitted with a mixed linear model including individual response curves as random term. In order to check if model assumptions were met, Q-Q plots or residuals and plots of residuals against predicted values were inspected. A "CF index" value was calculated as the difference between the mean ΔFt (stimulus) and the mean ΔFt (vehicle) in the last five minutes of ΔFt curve recording. Statistical analysis (analysis of variance) was performed to test if CF index values differ between phenotypic groups or between classes of CFTR mutation. Statistical significance was set at the level of $P<0.05$. Bonferroni procedure was used to adjust p-values when multiple tests were carried out. Analysis was performed with SAS 9.2 (SAS Institute, Inc., Cary, NC).

RESULTS

Detection of CFTR protein in human monocytes by western blotting

In epithelial cell lines, three forms of CFTR were detected: an incompletely-glycosylated form of CFTR with a molecular weight (MW) of approximately 130-140 kDa (band A), a partially-glycosylated form usually expressed by cells carrying two F508del mutations, with a MW of about 150 kDa (band B) and a fully glycosylated form with a MW of about 170-180 kDa. We obtained the same bands on human monocytes by western blotting. We used three antibodies, which recognize different epitopes present in all the three forms of CFTR described above (Fig. 5).

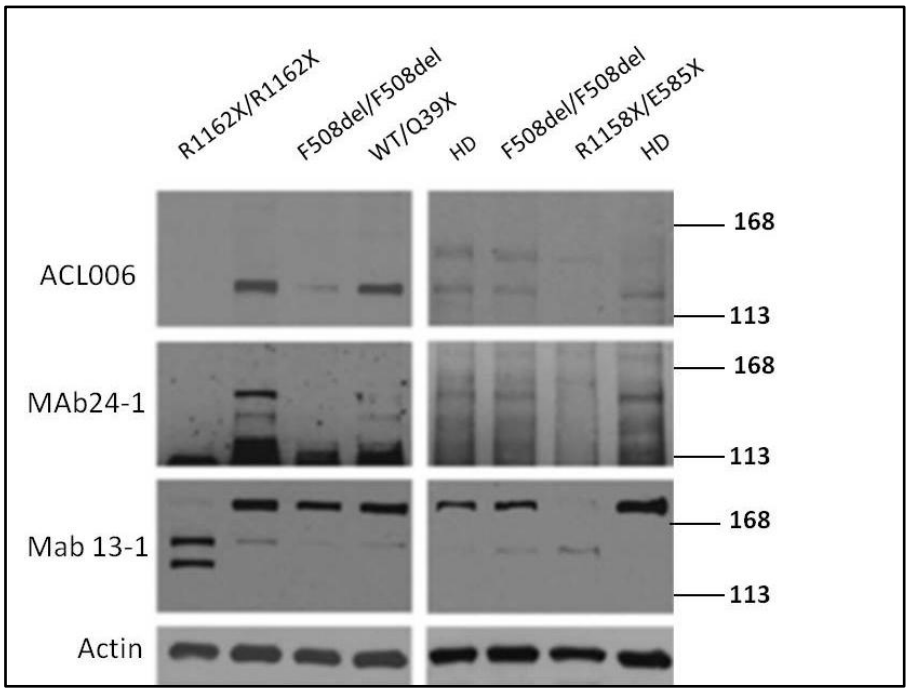

Fig.5 Western blotting on lysates of monocytes derived from patients with shown genotypes. Panel shows the result after incubation with anti-CFTR antibody ACL006, 24-1 or 13-1. All the CFTR form are detected in monocytes combinating all the antibodies. The bands corresponding to a full length CFTR present in healthy donors (HD) or obligate HTZ (WT/Q39X) are missing in monocytes derived from patients homozygous for nonsense mutations (13-1 antibody). Patients carrying one or two F508del alleles express a faint band. Actin expression is shown to demonstrate equal protein load

In contrast to epithelial cells, in monocytes the three bands of CFTR (A, B, C) corresponding to the CFTR forms were not detected by an individual antibody. Indeed, only a combination of all them allowed us to confirm the presence of all the differentially processed forms in human monocytes form Healthy Donors (HD): bands A and C were detected by ACL-006 antibody, band A and B by MAb 24-1 and band C by MAb 13-1. CFTR recognition was specific for all of these three antibodies since no signal was detected when appropriate controls were used.

Note that monocytes carrying two copies of a non-sense mutation (R1162X/R1162X) showed two bands when MAb 13-1 was used. The lower might correspond to a truncated form of CFTR since the antibody could recognize it according to the localization of its.

Since an isoform of CFTR (a MW of approximately 140 kDa) corresponding to a splice variant of the epithelial CFTR was detected in human cardiac muscle [88], analysis of CFTR mRNA was performed by RT-PCR to evaluate the possibility a lower molecular weight band was due to alternative splicing other than monocyte-specific post-translational processing (Fig.6).

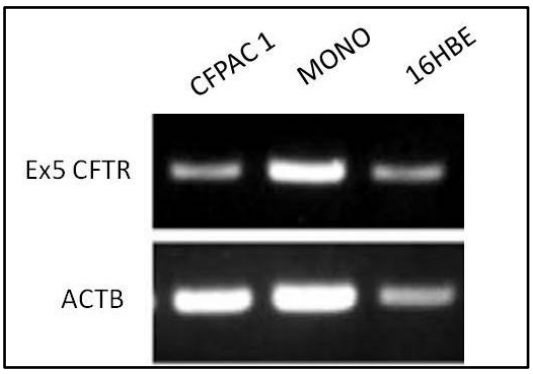

Fig.6. RT-PCR on epithelial cell, pancreatic adenocarcinoma cell line (CFPAC) and monocytes. mRNA detection confirmed the expression in monocytes of the same spliced isoform expressed in epithelial cells (16HBE) and CFPAC. As control was amplified actin (ACTB).

For this purpose primers located on exon4 and 6 were used. Results showed that monocytes express the same isoform as epithelial cells containing exon 5, which is excluded in the cardiac CFTR isoform.
Altogether these data indicate that monocytes express a full-length CFTR polypeptide, likely subject to cell-specific post-translational processing, and possess all the features necessary for a functional channel.

Detection of CFTR protein in lymphoblastoid cell line by western blotting

Both B and T lymphocyte cells are also involved in immune response in CF lung and, for this reason, they have been studied for many years. After immortalization of B lymphocytes by EBV, lymphoblastoid cell lines (LCLs) carrying different genotypes were obtained and the CFTR expression was detected by western blotting. Because of the low level of CFTR transcription in these cells, protein extract was immunoprecipitated with anti-CFTR antibody ACL-006 and then detected with MAb CF3 antibody (Fig.7), which recognizes an extracellular epitope of CFTR.

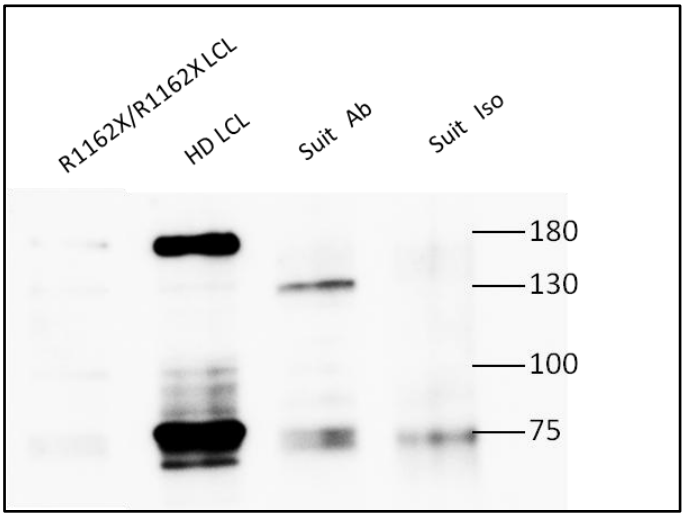

Fig.7 Western blotting on lysates of pancreatic adenocarcinoma cell line and lymphoblastoid cell lines. CFTR was immuno-purified from lysates of pancreatic adenocarcinoma cell line (Suit-2) and lymphoblastoid cell lines using anti-CFTR antibody ACL006. CFTR was detected using anti-CFTR antibody CF3 as a specific band at about 180 kDa in cell line obtained from HD. The same band was missing in cell line derived from patients homozygous for nonsense mutations (R1162X/R1162X). A band a lower MW was detected in HD at approximately 90-100kDa. Suit-2 was used as positive control. The band was not detectable when immune precipitation was performed with isotypic antibodies

The most glycosylated CFTR isoform was detected in LCL obtained from HD, whereas LCL carrying two non-sense mutations (R1162X/R1162X) did not show any band corresponding to CFTR protein. The same band was not detected when immunoprecipitation was performed with isotopic antibody confirming the specific correspondence of the band to CFTR protein.

Moreover, a band with lower MW than that corresponding to any of the major forms of CFTR was detected in HD lymphoblastoid cells at approximately 90-100 kDa (Fig.8).

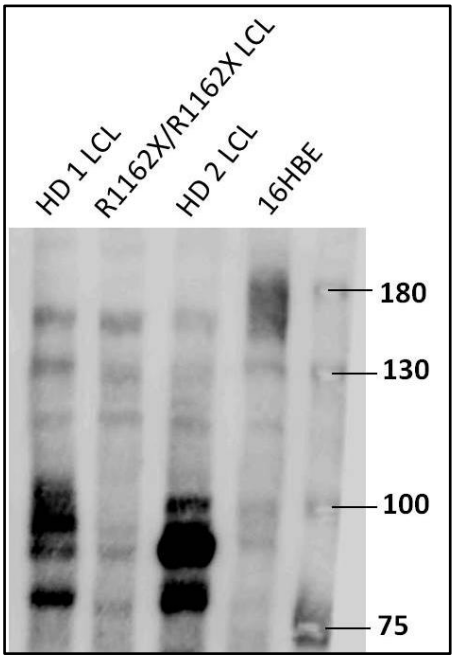

Fig.8 Western blotting on lysates of epithelial cell line and lymphoblastoid cell lines. A band at about 90-100 kDa was detected using anti-CFTR antibody ACL006 in cell line obtained from HD. The same band was missing in cell line derived from patients homozygous for nonsense mutations (R1162X/R1162X). Epithelial cell line (16HBE) was used as positive control.

Quantitative analysis of CFTR mRNA in LCLs

Some LCLs carrying different genotype were analyzed by real time RT-PCR (Table1).

Genotype	CFTR	GAPDH	$2^{-\Delta\Delta C}{}_T$
HD	31.94	17.95	1.00
HTZ (F508del)	34.60	19.43	0.44
HTZ (F508del)	33.79	17.58	0.22
R1162X/R1162X	31.64	17.71	1.04
G542X/R553X	36.01	17.13	0.03
R1162X/R1162X	33.65	17.11	0.17
F508del/R1158X	34.93	17.42	0.09
F508del/R1158X	35.54	16.75	0.04
Cell lines			
16HBE	17.94	17.32	1.00
IB3	33.94	16.07	0.00

Table 1 CFTR mRNA analysis by Real-Time PCR mRNA fold change of CFTR quantified by RT-*q*PCR in LCLs from CF patients versus non-CF subjects and in IB3 versus 16HBE cell lines using GAPDH as housekeeping gene. Relative quantification was performed using the $\Delta\Delta C_t$ method.

The following LCLs were analyzed: HD, LCL F508del mutation only in one allele (HTZ F508del), LCLs carrying two different pairs of two non-sense mutations (R1162X/R1162X and G542X/R553X) and a LCL carrying F508del mutation on one allele and class I mutation on the other allele. GAPDH was used as housekeeping gene and two different epithelial cell lines as positive (16HBE) and negative control (IB3). As expected, differences were observed between non-CF LCL and CF LCL groups as observed in epithelial cell lines. Precisely, CF LCL showed a lower level of CFTR mRNA than that observed on HD LCL. Note that only one LCL carrying two R1162X/R1162X mutations (lane 4 of the table) showed a higher level of CFTR mRNA than that observed in other LCL having the same genotypes. This may be explained by a different regulation of mutant mRNA degradation machinery.

Flow cytometry assay to evaluate the expression of CFTR protein in monocytes and LCLs

Using human whole blood, monocytes form HD and CF patients were identified as CD14 positive cells (Fig.9) by flow cytometry technique.

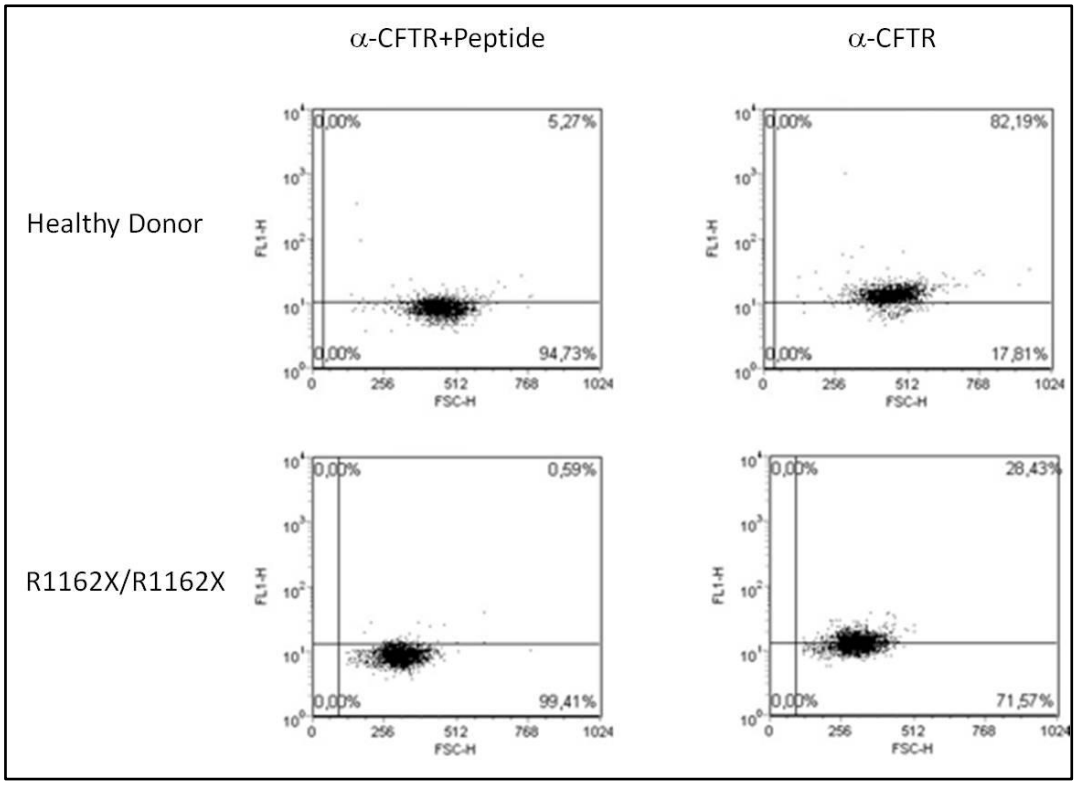

Fig.9 CFTR expression in human monocytes by Flow Cytometry assay. CD14 positive cells were identified and a threshold of CFTR-signal (red line) was set to obtain 90-98% of total monocytes, stained with blocking peptide pre-incubated anti-CFTR antibody (α-CFTR+Peptide), below the value. Events above the threshold were considered background noise. The same subject's monocytes, incubated with the anti-CFTR antibody without the peptide (α-CFTR), were then registered and a percentage of monocytes having a signal above the threshold was obtained.

Two different conditions were performed: blood sample was incubated either with anti-CFTR antibody ACL-006 pre-incubated with a blocking peptide (α-CFTR+Peptide) or, in the other condition, with the anti-CFTR antibody ACL-006 without the peptide (α-CFTR). The first condition was used to set a threshold of the highest signal, whereas events above the threshold were considered background noise. In this way, it was possible to obtain a value of percentage of monocytes having a signal above the threshold (CFTR positive) as well as a geometrical mean of the signal of monocytes stained under the two conditions. Finally, mean fluorescence intensity (MFI) was calculated as a ratio between the geometrical means of the two conditions.

The study was performed using different groups of mutation classes. The percentage of CFTR positive monocytes and MFI values were used to compare them (Fig.10).

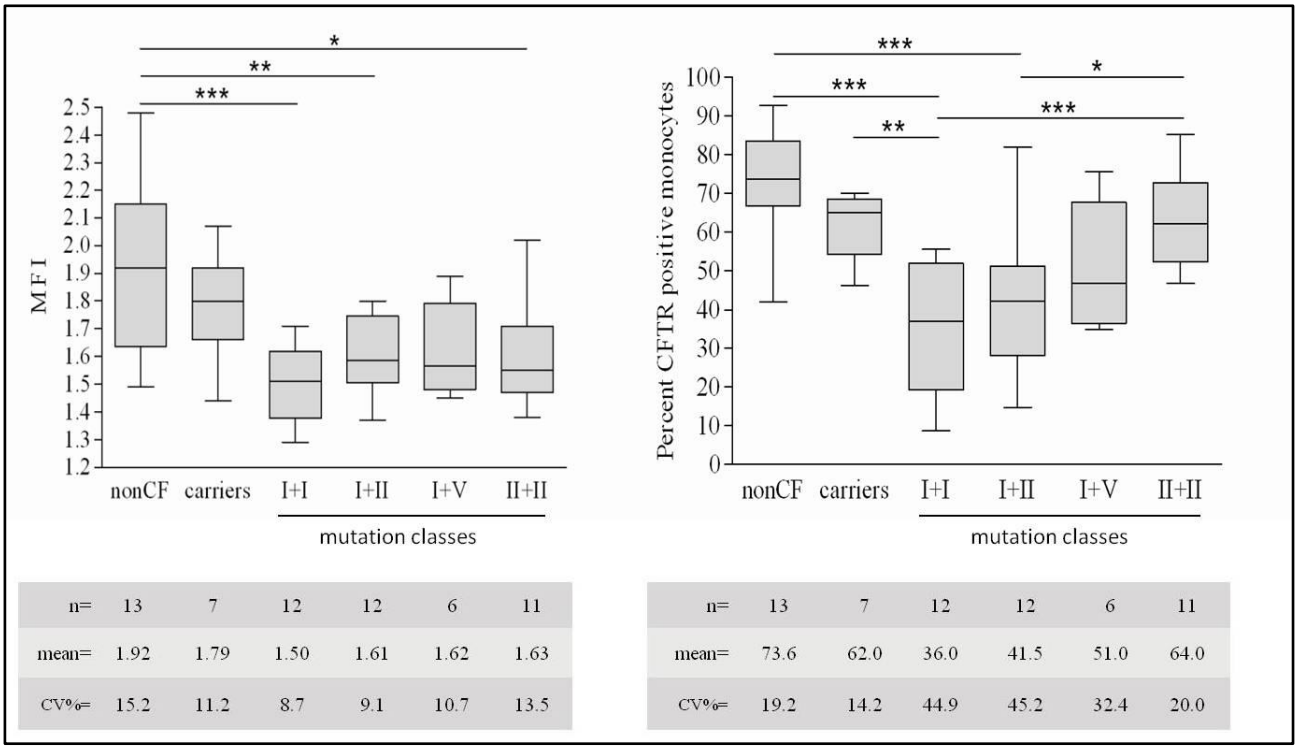

	nonCF	carriers	I+I	I+II	I+V	II+II
n=	13	7	12	12	6	11
mean=	1.92	1.79	1.50	1.61	1.62	1.63
CV%=	15.2	11.2	8.7	9.1	10.7	13.5

	nonCF	carriers	I+I	I+II	I+V	II+II
n=	13	7	12	12	6	11
mean=	73.6	62.0	36.0	41.5	51.0	64.0
CV%=	19.2	14.2	44.9	45.2	32.4	20.0

Fig.10 Statistical analysis of flow cytometry data of monocytes. MFI and % of monocytes were calculated and a one-way ANOVA was used to compare means between groups of mutation classes. class I+I and II+II =subjects with class I or class II mutations on both *CFTR* alleles; class I+II and I+V=subjects with class I mutation on one allele and class II or class V mutation on the other allele; carrier= subject with a mutation on only one allele; CV= coefficient of variation; n= number of subjects in each group. Differences between MFI values and %-values could be observed, however %-values demonstrated greater variability. P<0.001, ***; p<0.05, **; p<0.01, *

The studied groups were: non-CF subjects, healthy carriers, CF subjects with class I or class II mutations on both *CFTR* alleles (I+I and II+II respectively) and CF subjects with class I mutation on one allele and class II or class V mutation on the other allele (I+II and I+V respectively). Comparing CF groups to non-CF group, we observed lower MFI values in I+I, II+II and I+II groups. On the other hand healthy carriers did not show MFI values statistically different from any group.

Flow cytometry assay was also used to study CFTR expression in LCLs (Fig.11).

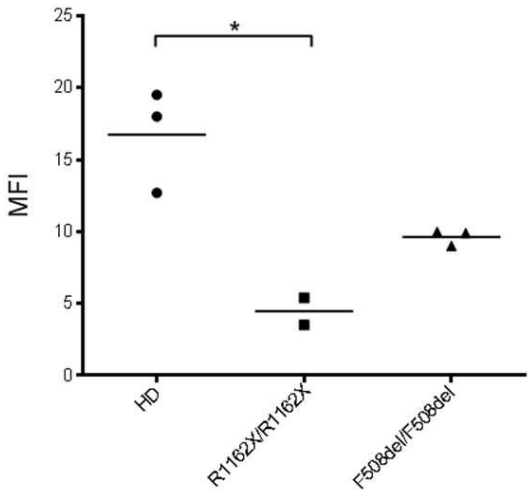

HD	R1162X/R1162X	F508del/F508del
19,51	3,50	9,97
12,70	5,40	9,90
18,00	*14,00**	9,00

Fig.11 Distribution of MFI of lymphoblastoid cell lines using flow cytometry assay. MFI were calculated on living cells of lymphocytes cell lines obtained from HD and patients carrying two non-sense or two F508del mutations. Differences value were obtained according to genotype and statistically difference was observed when HD group was compared to R1162X/R1162X group (p=0.01, *). Table show the MFI values calculated for each LCL in each group. In the group of cell lines carrying two non-sense mutations, only one cell line showed a high MFI value: maybe, it could express a truncated form of CFTR.

CF3 antibody (MAb CF3) was used to stain cells. Living cells were identified using Vybrant Dye Cycle stain, which emits a fluorescence signal after binding DNA. Geometrical means of the signal emitted from the secondary antibody linked to anti-CFTR antibody CF3 was obtained using two conditions: cells stained with MAb CF3 and cells stained with IgM isotope control. MFI was then calculated and expressed as a ratio between the two geometrical means.

Three groups of LCLs were compared: HD group, LCL with two non-sense mutations and LCL with two copies of F508del mutation. Statistic significant was observed comparing HD LCL with R1162X/R1162X LCL, but the number of LCL analyzed should be increased in order to obtain better statistics.

Table (Fig.11) summarizes the MFI values calculated for each LCL in each group. Only one LCL of the R1162X/R1162X group showed a higher MFI value than other ones. This cell line was the same that had the highest CFTR mRNA level consistent with possibility of detection of CFTR truncated form in that LCL.

Membrane localization of CFTR protein on monocytes and lymphoblastoid cells

Confocal microscopy assay was used as a technique to localize CFTR protein on monocytes (Fig.12) and LCLs (Fig.13).

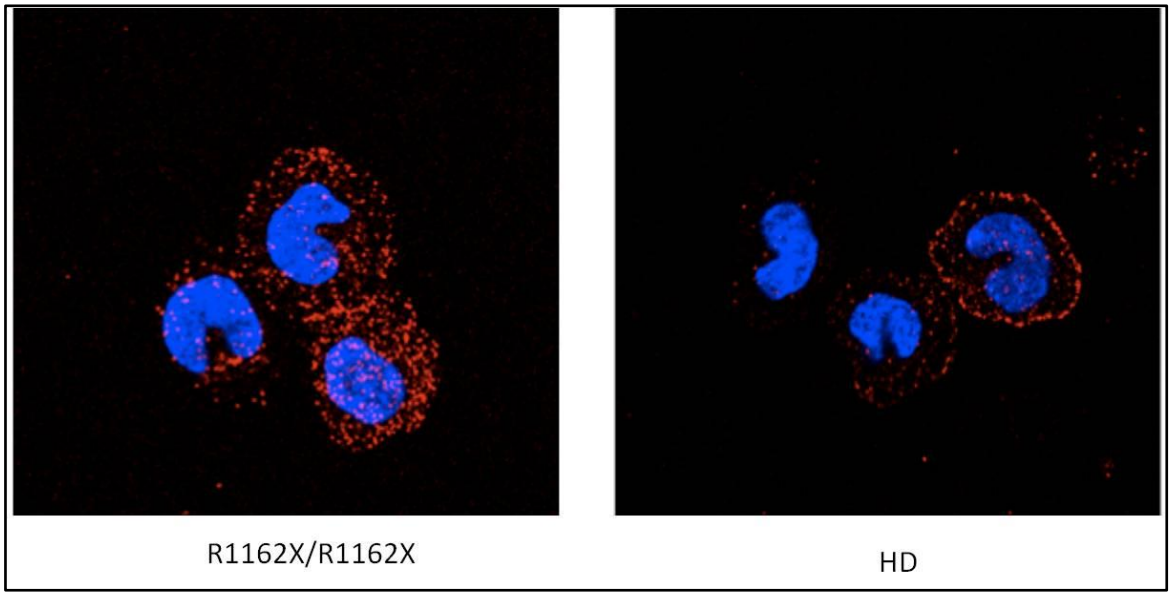

Fig.12. CFTR expression on monocytes by confocal analysis. Assay was performed using the anti-CFTR antibody 13-1 on monocytes derived from subjects carrying a truncated (R1162X/R1162X) and from HD. Membrane distribution was revealed in HD monocytes, while R1162X/R1162X ones display a red spots inside cell corresponded to truncated CFTR form. The panel show one experiment of three performed.

Staining by MAb 13-1 antibody on non-CF monocytes confirmed at membrane localization of CFTR protein which was lost in monocytes isolated from patient carrying two R1162X/R1162X mutations. On the other hand, red spots spread into the cytoplasm were observed in monocytes from the patient. These spots could correspond to a truncated form of the CFTR protein as confirmed by western blot data (Fig.5).

Membrane localization was also detected on LCLs (Fig.13).

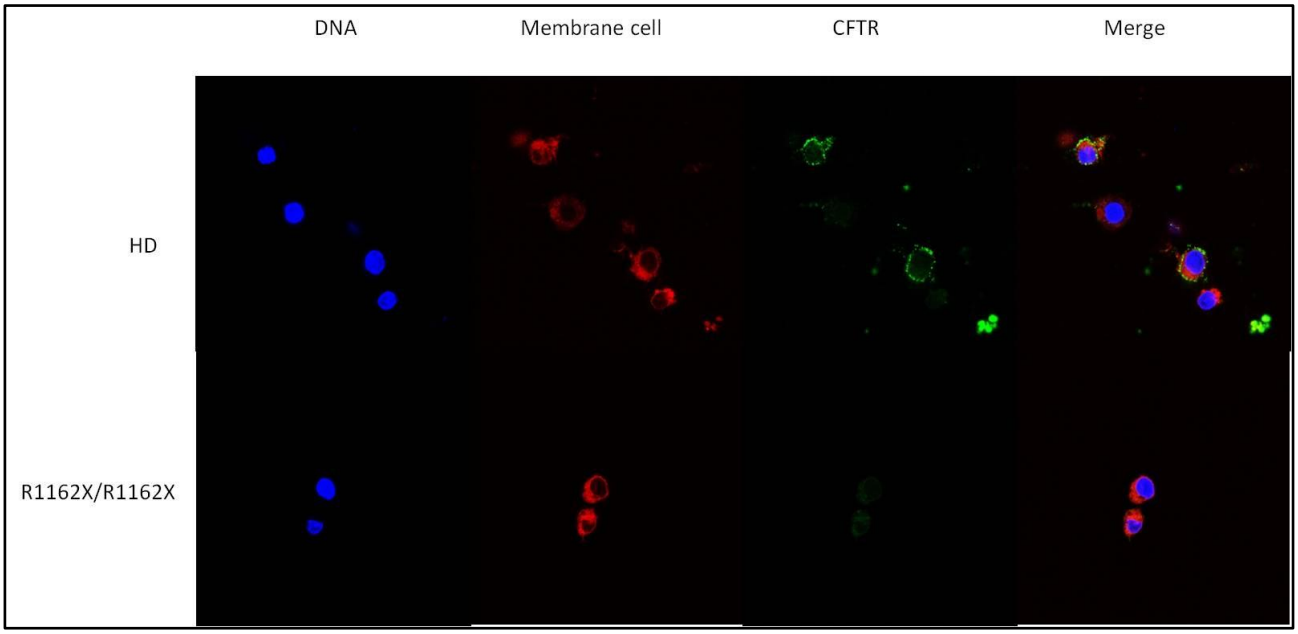

Fig.13 CFTR expression on LCLs by confocal analysis. Assay was performed using the anti-CFTR antibody CF3 on LCLs carrying two non-sense mutations (R1162X/R1162X) and HD LCLs. Membrane localization was detected on HD cell line which was lost on R1162X/R1162X cell line. Blue colour=TO-PRO3, nuclear stain; Red colour:=Cell Mask Orange, plasma membrane stain; Green colour= antibody CF3.The panel show one experiment of three performed.

The staining was performed using MAb CF3 as anti-CFTR antibody (green signal), To-PRO3 as specific nuclear stain (blue signal) and Cell Mask Orange as plasma membrane stain (orange signal). A perfect overlapping between green and orange signal was observed on HD cells, whereas on cells with R1162X/R1162X genotype the green signal disappeared confirming the undetectable levels of CFTR protein on plasma membrane.

Evaluation of CFTR functional activity on human monocytes by single cell imaging assay

Functional activity of CFTR in monocytes was evaluated by single-cell fluorescence imaging technique which is based on membrane potential (Vm) changes in single cells. The Vm is measured using a potential-sensitive fluorescent probe called bis-(1,3-diethylthiobarbituric acid) trimethine oxonol ($DiSBAC_2(3)$) [87]. It is a slow-response probe, which enters depolarized cells and binds to intracellular protein or membranes and this enhances fluorescence emission. That is, a membrane depolarization results in additional influx of the anionic dye and an increase in fluorescence. The method is quick, simple and reproducible and does not require any cell loading procedure.

After setting up the method using pancreatic cells such as Suit-2 and CFPAC [89], membrane depolarization induced by stimulus (8-Br-cAMP, IBMX and Forskolin) was measured in monocytes (Fig.14).

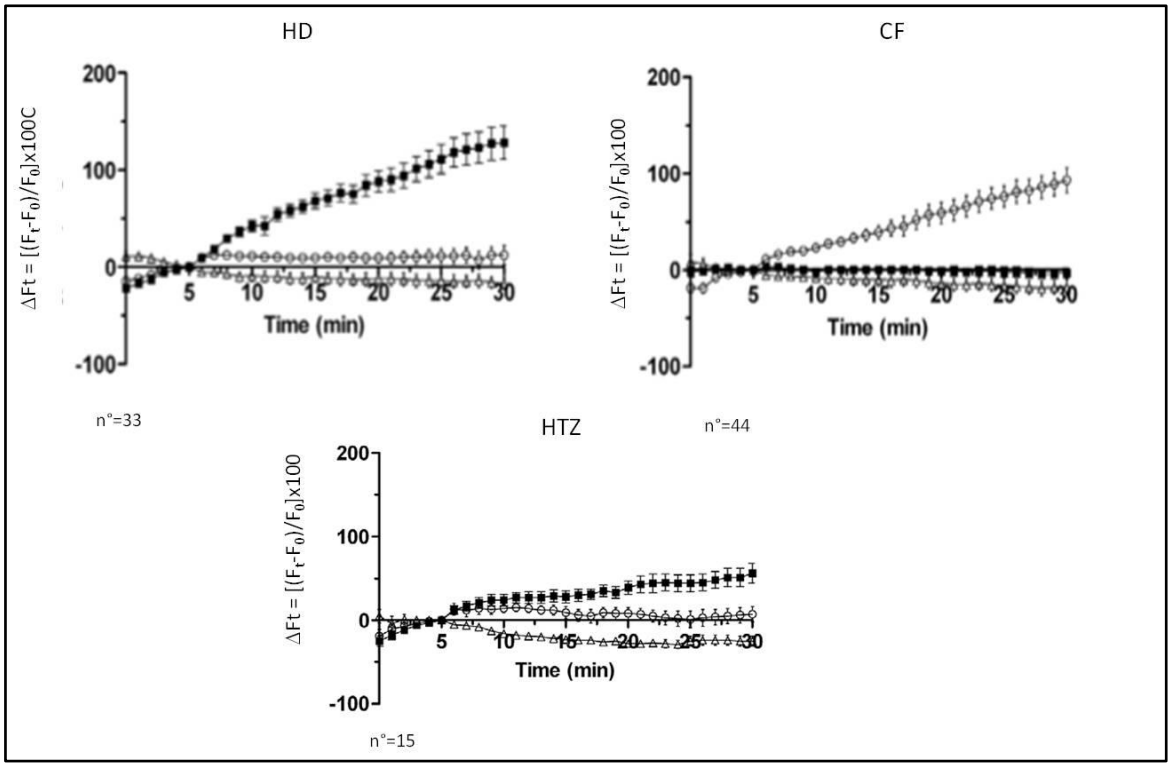

Fig.14 CFTR function analysed by single-cell fluorescence imaging assay on human monocytes. Fluorescence variation (ΔF) of $DiSBAC_2(3)$ was represented as $\Delta Ft = [(F_t-F_0)/F_0]x100$, where F_t and F_0 are the fluorescence values in absence of extracellular Cl^- at time t and at the time of addition of the stimulus respectively. A mean ΔFt and standard error were calculated and represented in these graphs. The left graph corresponds to walk of non-CF human monocytes, the right graph corresponds to CF human monocytes and the central graph corresponds to HTZ monocytes. Black square= stimulus (8-Br-cAMP/forskolin/IBMX); White triangle=stimulus+ CFTR inhibitor (CFTR(inh)-172); White ball=vehicle

In monocytes belonging to non-CF group (left graph), stimulus induced a rapid fluorescence increased (black square in the graph), which was completely inhibited by a specific CFTR(inh)-172 [90] (white triangle in the graph). As expected, monocytes from subjects carrying only one mutation on one allele (HTZ) responded to stimulus with an increase fluorescence, but it was lower than that observed in non-CF cells (central graph). On the other hand, monocytes obtained from CF patients (right graph) showed a decrease of the baseline fluorescence signal in response to the stimulus (black square in the graph). Moreover, the control baseline recorded in the presence of vehicle alone (white ball) increased, corresponding to a spontaneous depolarization, which was inhibited using amiloride. The latter is able to block Na^+ channel activity that is higher in CF cells than in non-CF. The use of amiloride suggests the involvement of Na^+ channels in membrane depolarization of CF monocytes.

For better defining the differences between groups, we calculated an index, called "CF-index", expressed as the difference between fluorescence variation after stimulation (ΔF_t) and fluorescence variation in presence of vehicle alone (ΔF_0).

The CF-index values were clustered for groups and a distribution of data in the three phenotypic groups was obtained (Fig.15).

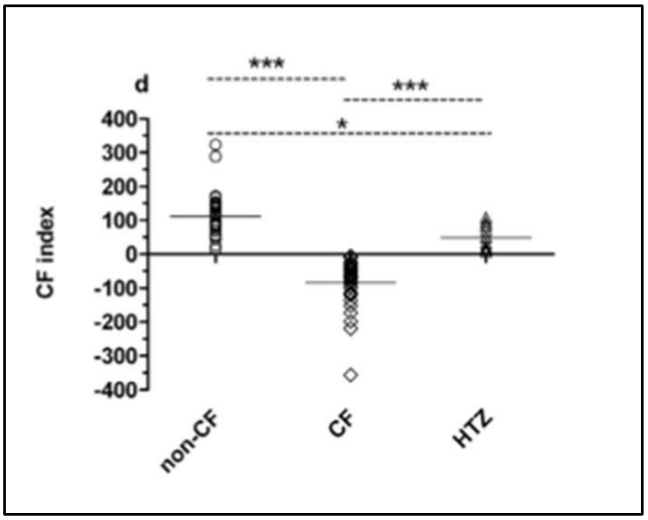

Fig.15 Statistical analysis of fluorescence data between groups. CF-index was calculated as difference between the maximum fluorescence value obtained under stimulation and the matching fluorescence value of vehicle. Difference statistically significant was observed between CF and non-CF group ($p<0.001$, ***), between CF and HTZ group ($p<0.001$, ***) and between HTZ and non-CF group ($p=0.015$, *).

The CF-index values in the CF group were lower than those of HTZ and non-CF group ($p<0.0001$ in both cases). Also, the difference observed between non-CF and HTZ groups was significant ($p<0.01$), but was not considered appropriate for using CF-index to discriminate between these groups due to the still insufficient sample size.

NPD versus functional test of monocytes

For proposing a single-cell fluorescent assay as a functional CFTR test, the method basted on monocytes was compared to the NPD diagnostic test, which measures CFTR activity in vivo recording Voltage magnitude (Vm) on epithelial cells of the upper respiratory tract (Fig.16).

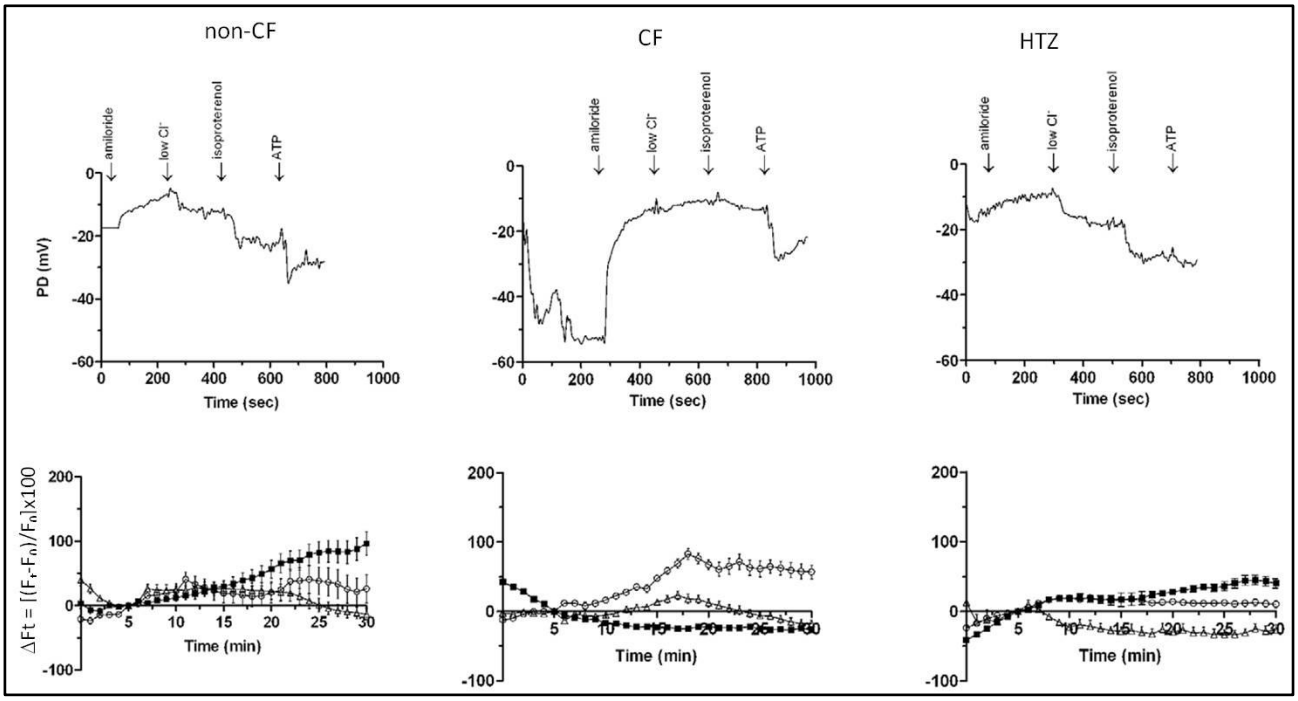

Fig.16 NPD analysis compared to single-cell fluorescence imaging assay. Upper panel: common NPD measurements of non-CF subject (left graph) and CF patient (right graph). The arrows indicated the time at the respective solution was added. Non-CF and HTZ subjects showed a response to Cl^- free solution and isoproterenol, while CF patients showed a higher depolarization in presence of amiloride. ATP has been utilized as a stimulus for alternative non-CFTR Cl^- secretory pathways as Ca^{2+} activated Cl^- channels. Bottom panel: fluorescence variation analysis on monocytes obtained from the same subjects tested by NPD. Also during this analysis, a fluorescence increase in response to stimulus was observed in non-CF and HTZ groups but not in CF subjects. Black square= stimulus (8-Br-cAMP/forskolin/IBMX); White triangle=stimulus+CFTR(inh)-172; White ball=vehicle

Some subjects participating in the functional study of monocytes were also tested by NPD measurements. The NPDs tracings resulted to be consistent with the fluorescence variation tracings recorded in monocytes of the same subject. Indeed, in non-CF individuals, stimulus-induced increase of fluorescence corresponded to increased NPD, whereas in CF patients, little or no changes in the NPD after addition stimulus matched to no variation of fluorescence in single-cell fluorescence imaging.

Moreover, amiloride effects on spontaneous depolarization of control baseline observed in CF monocytes was consistent to increased potential difference detected when amiloride solution was perfused into nostril of CF patients.

In the HTZ group, increased polarization is induced by Cl^- free solution and isoproterenol in the presence of functional CFTR as in non-CF, but the increase was less marked. The same results were observed in single-cell fluorescence tracings where the fluorescence increased following stimulation was substantially lower than that detected in non-CF monocytes (Fig.14, central graph).

Evaluation of CFTR functional activity in LCLs by single-cell fluorescence assay

Single-cell fluorescence technique was applied on LCLs for studying CFTR activity. Two phenotypic groups were studies: LCLs from HD and LCLs from CF patients carrying two non sense mutations.

As monocytes, the membrane depolarization was induced using stimulus (8-Br-cAMP, IBMX and Forskolin) and the control baseline was recorded after addition of vehicle alone (Fig.17).

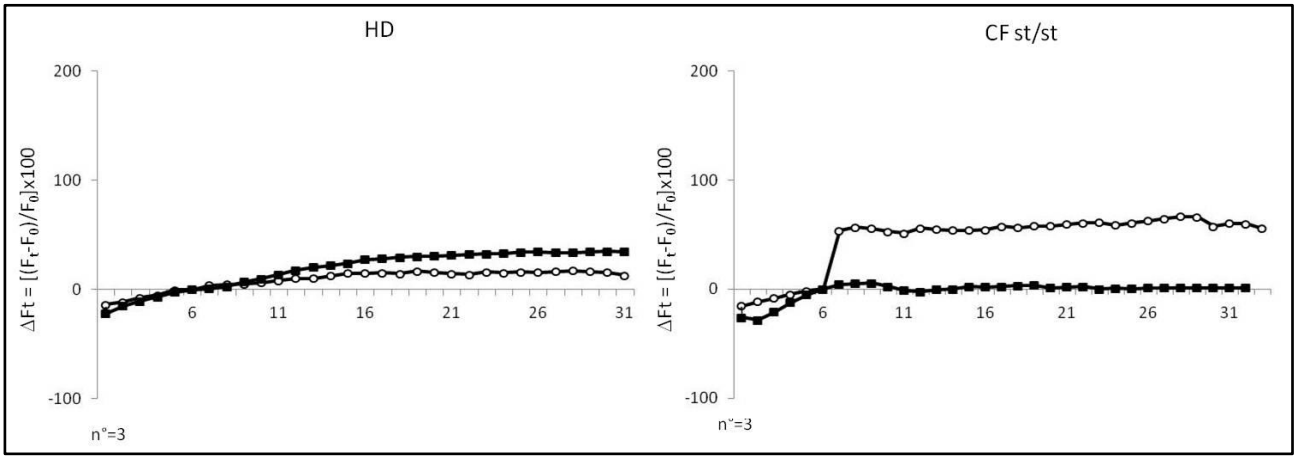

Fig.17 CFTR function analysed by single-cell fluorescence imaging assay on LCLs. Fluorescence variation (ΔF) of $DiSBAC_2(3)$ was represented as $\Delta Ft = [(F_t-F_0)/F_0]x100$, where F_t and F_0 are the fluorescence values in absence of extracellular Cl^- at time t and at the time of addition of the stimulus respectively. A mean ΔFt and standard error was calculated and represented in these graphs. On the left graph it was represented the fluorescence variation of HD lymphoblastoid cell lines, while on the right graph that of CF lymphoblastoid cell lines carrying two non sense mutations. Black square= stimulus (8-Br-cAMP/forskolin/IBMX)+CFTR(inh)-172; White ball=vehicle+Amiloride

Also in these cells, non-CF cells showed an increase of membrane depolarization in response to stimulus, whereas in the CF group the fluorescence signal did not increase. On the other hand, the latter cell lines exhibited spontaneous depolarization with vehicle alone. These data confirm a defect in the membrane conductance as we noted in monocytes.

The CF-index distribution (Fig.18) was also obtained and statistical analysis showed a significant difference between the two groups. Surely, the number of observations in each group should be increased to gain better statistics.

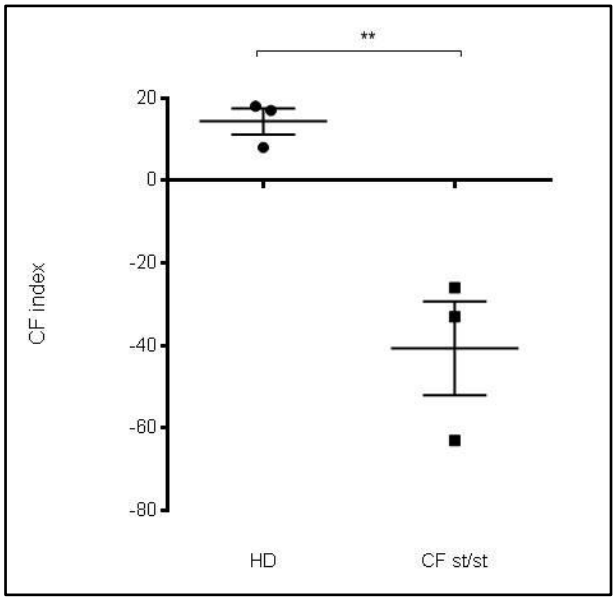

Fig.18 Analysis of fluorescence data between LCLs groups. CF-index was calculated as difference between the maximum fluorescence value obtained under stimulation and the matching fluorescence value of vehicle. Statistical difference was observed when two groups were compared ($p<0.005$, **)

DISCUSSION

Inflammation in CF is a hallmark of the disease and the causative event associated to the negative outcome of these patients that almost invariably suffer and eventually die because of chronic pulmonary disease. Identification of all the players in this complex scenario is mandatory to approach this lethal disease and develop effective therapeutic protocols.

We focused our attention to monocytes demonstrating expression and functional activity of the CFTR channel in these cells. We also aimed to describe a functional test useful to evaluate CFTR activity and to distinguish non-CF from CF subjects in a rapid, reproducible and easier than others currently used tests in CF diagnosis.

Of interest is the observation that monocytes express the CFTR protein in all the known CFTR forms as epithelial cells do, though we needed a combination of three different antibodies to detect them. The loss of the bands in patients with two non-sense mutations known to affect CFTR protein expression confirmed the specificity of the results. A previously described alternatively spliced isoform, which miss exon 5 was demonstrated not to be expressed in these cells. Furthermore, the membrane localization of CFTR Cl^- channel was confirmed in human monocytes.

CFTR expression in monocytes was also evaluated using flow cytometry with results described by % of CFTR-positive cells and MFI values to compare monocytes with different genotypes. This procedure for studying CFTR protein expression has been already applied in primary human nasal brushing epithelial cells [91] demonstrating that CF patients express total CFTR protein levels that are significantly reduced compared to HDs. These authors used an internal standard to correct for variation in staining intensity between brushing obtained at different days. In our setting monocytes, we utilized peptide competition as proper control, a procedure that allows us to compare data among donors. Furthermore, monocytes are present in suspension and are less subject to variability during the preparation.

In our evaluation, we need to consider that the % of positive cells measure the % of the total cell number that exceed the value obtained using the competing peptide, regardless of the intensity of the signal that is evaluated by MFI value. As such it is not surprising that, although the MFI is low in all CF subject, as expected by the loss or the incompletely processing of CFTR protein in CF, the % of positive cells increased in carriers of type I mutations. Indeed, intracellular accumulation of CFTR is a feature of mutations other than non sense (such as type I) and intracellular staining is therefore contributing to an albeit low signal associated to the majority of the cells expressing partially degraded CFTR, as expected in cells that are not homozygous for non-sense mutations.

Flow cytometry analysis of relative CFTR expression levels offers important advantages over conventional approaches to study CFTR expression in patient samples such as western blotting and mRNA analysis. Flow

cytometry analysis required few cells for analysis, short procedures and the absence of enzymatic procedures to detect CFTR-bound antibodies. The variability of the staining in these cells is still present and further studies utilizing antibodies reacting against alternative epitopes might be helpful to improve the reproducibility and reduce the variability of the measures.

Another important step in this work was to study the CFTR Cl^- channel activity in human monocytes. During my PhD work, I have contributed to set up a new functional test [89] by devising an index, which was able to distinguish between non-CF and CF groups. Although other functional tests, such as ST, NPDs measurement and ICM, are currently used for diagnostics, none of these are able to identify heterozygous carriers of CFTR mutations, suggesting that this assay is indeed measuring a CFTR-specific defect in these cells. However, statistical analysis requires an increased number of subjects in the HTZ group in order to gain a better discrimination between the groups.

The exact role of CFTR in monocytes is yet unidentified. On the other hand the role of macrophages has been studied for years and their involvement in the CF inflammatory process has been reported [92]. Since monocytes differentiate into macrophages in response to inflammation signals, we might suppose a role of monocytes in the CF pathophysiology.

Comparing this test performed on monocytes with NPD, we observed a clear concordance between both technique demonstrating a similarity between epithelial cells and monocytes. We also applied monocyte test on difficult cases, such as a patient who has ST borderline value and one or two unknown mutations. In this case we could support a diagnosis of CFTR (having measured a negative CF index) that was in agreement with Wilschanski's index (>0.70) [93] calculated based on of NPD. Thus, the monocytes functional test appears to be capable to support clinical diagnosis of CF also in difficult cases.

Each diagnostic test is usually not performed alone. Indeed, ST is often coupled with NPD and ICM to diagnose CF in atypical cases. So, pending additional tests, we might propose in the future monocytes functional test as a minimally invasive procedure that can complement and potentially replace other functional tests commonly used in diagnostics.

Another blood test has been described to be useful in the diagnosis of CFTR related diseases [94, 95]. This test utilizes red blood cells (RBCs) following previous findings that demonstrated the presence of CFTR in RBCs, its role in Cl^- ion transport and interaction with other membrane proteins along with their role in ATP release [96] [97]. The authors used RBC plasma membrane from HDs and from CF patients and combined the immunostaining to atomic force microscopy (AFM) to allocate a specific protein within the membrane. The combination of fluorescence microscopy and AFM revealed that human RBCs have a CFTR distribution similar to that of epithelial cells as well as disclosing a reduced number of CFTR molecules in cells derived from CF patients compared to healthy individuals. These authors proposed to apply this technique to quantify and localize CFTR protein and to study its dynamics within native membrane at a single-molecule level.

Specific CFTR function in RBC is still unknown. Apart from mild hemolytic anemia due to reduced antioxidative defense in CF patients [98], there are no major hematological disorders reported for patients with cystic fibrosis. Since lung disease is the main cause of death and hyper-inflammatory status (a leukocyte-based disorder) is a hallmark of CF, monocytes might well be correlated with the pathophysiology of CF.

Another potential application of the monocytes assays could be in translational research. These cells might represent a valuable marker of the therapeutic effects of CFTR-targeted drugs in CF patients and the test might be used to evaluate their efficiency on correcting CFTR function.

Focusing on this point, a better cellular model to study effects and efficacy of drugs targeting mutations affecting CFTR expression and function may be LCLs obtained from B cells of healthy individuals and CF patients. The application of these cell lines in CF research is not new. Previous findings demonstrated the use of these cells for evaluating the in vitro effect of five antibiotics at sub-inhibitory concentrations on the adhesive properties of *Pseudomonas aeruginosa* isolated from cystic fibrosis sputa [99].

We characterized the LCLs applying the same techniques used on monocyte to analyze the expression and function of the CFTR Cl^- channel. We confirmed the presence of the fully glycosylated isoform of CFTR in LCLs not carrying any mutation and we observed a fragment of CFTR at about 90-100 kDa, which might be generated through processing of native CFTR by calpain activity as Averna M. et all demonstrated in their studies. These authors showed a direct relationship between the accumulation of the CFTR fragments of about 100 kDa and 70 kDa and calpain activity in circulating human lymphocytes [100]. The same band was also detected in HD lymphoblastoid cell line with another antibody ACL-006 (Fig. 8) and was absent in an epithelial cell line (16HBE) that, in contrast, expressed CFTR isoform B and C. All these results support the hypothesis that the band at about 90-100 kDa could correspond to one fragment of CFTR generated by calpain activity. This issue could be addressed by blocking calpain activity by the addition of the protease inhibitor C.I.2 or by promoting intracellular calpain activity loading the cells with Ca^{2+}.

Flow cytometry assay also revealed information about CFTR expression in LCLs. MFI values allowed us to distinguish LCLs originating from healthy individual from those originating from CF patients making sturdier the hypothesis to use this test to detect CFTR level changes.

Furthermore, single-cell imaging allowed us to study functional activity also in LCLs. Cell lines carrying two non-sense mutations did not respond to stimulus, just as we observed in monocytes having the same genotype. A negative CF-index was associated to a CF genotype, just like when using monocytes, allowing us to distinguish between healthy and CF LCLs. All these results help to understand the benefit of our functional test in a clinical field.

LCLs might be useful also to study new mutations and their effects on the CFTR gene. Lymphoblastoid cells have been already used to study alternatively spliced transcripts of the CFTR gene [3] and effects of a specific nucleotide substitution (1898+5G>T) on mRNA [101].

Moreover, lymphoblastoid cells are more easily accessible than monocytes or other immune cells, as growing indefinitely, they do not require patient's collaboration for more than once. All these features make the LCLs an attractive cellular model to study the CFTR channel in all of the individual patients' variants.

In conclusion we have shown that the study of leukocytes can find various application in the field of CF, starting for the basic science and leading to clinical applications. Future studies will reveal whether this approach will find its way in these fields and contribute to improve our understanding of the disease and improve patients' management.

ACKNOLEDGMENT

Foremost I would like to express my gratitude to my supervisor Dr. Paola Melotti for the continuous support of my PhD study and research, for her patience, motivation and knowledge.

I also would like to thank Dr. Claudio Sorio for having helped me in all of the research and of the writing of this thesis and for his encouragement and insightful comments.

I thank my fellow labmates Jan Johansson, Chiara Angiari, Gabriella Bergamini, Elisabetta Moratti and Angela Sandri for the absolute support for the thesis and for the support and encouragement whenever I was in need.

I thank my colleagues at the Cystic Fibrosis Center, Laura Menin and Elisa Calcaterra, for their technical assistance to my project.

I am thankful to Franco Olivetti for his selfless support, encouragement, and love given to me during the course of this thesis.

Finally, I take this opportunity to express my profound gratitude to my beloved parents and to my sibling for their love and continuous support. I also would like to thank my little nieces, Noemi and Matilde, for the laughters gifted to me with their cute and tender voices. This thesis would also have not been possible without the love and support of all of them which instilled within me a love of creative pursuits, science and language, all of which find a place in this thesis.

This study was supported by the Italian Cystic Fibrosis Research Foundation.

REFERENCES

[1] Chen JH, Schulman H, Gardner P. A cAMP-regulated chloride channel in lymphocytes that is affected in cystic fibrosis. Science. 1989;243:657-60.

[2] Brickell PM. Immortalization of human B-lymphocytes by epstein-barr virus. Methods Mol Biol. 1992;8:213-8.

[3] Bienvenu T, Beldjord C, Chelly J, Fonknechten N, Hubert D, Dusser D, et al. Analysis of alternative splicing patterns in the cystic fibrosis transmembrane conductance regulator gene using mRNA derived from lymphoblastoid cells of cystic fibrosis patients. European Journal of Human Genetics. 1996;4:127-34.

[4] Maler T, Riordan JR. Isolation and characterization of the plasma membranes of cultured lymphoblasts from patients with cystic fibrosis and normal individuals. Biochim Biophys Acta. 1980;598:1-15.

[5] Walters SM. Epidemiology of Cystic fibrosis. In: Hodson M, Geddes DM, A B, editors. London2007.

[6] Yamashiro Y, Shimizu T, Oguchi S, Shioya T, Nagata S, Ohtsuka Y. The estimated incidence of cystic fibrosis in Japan. J Pediatr Gastroenterol Nutr. 1997;24:544-7.

[7] Sferra TJ, Collins FS. The molecular biology of cystic fibrosis. Annu Rev Med. 1993;44:133-44.

[8] Mehta A. CFTR: more than just a chloride channel. Pediatr Pulmonol. 2005;39:292-8.

[9] Vankeerberghen A, Cuppens H, Cassiman JJ. The cystic fibrosis transmembrane conductance regulator: an intriguing protein with pleiotropic functions. J Cyst Fibros. 2002;1:13-29.

[10] Quinton PM. Cystic fibrosis: impaired bicarbonate secretion and mucoviscidosis. Lancet. 2008;372:415-7.

[11] Rowe SM, Miller S, Sorscher EJ. Cystic fibrosis. N Engl J Med. 2005;352:1992-2001.

[12] Lubamba B, Dhooghe B, Noel S, Leal T. Cystic fibrosis: insight into CFTR pathophysiology and pharmacotherapy. Clin Biochem.45:1132-44.

[13] Gibson LE, Cooke RE. A test for concentration of electrolytes in sweat in cystic fibrosis of the pancreas utilizing pilocarpine by iontophoresis. Pediatrics. 1959;23:545-9.

[14] Kerem B, Rommens JM, Buchanan JA, Markiewicz D, Cox TK, Chakravarti A, et al. Identification of the cystic fibrosis gene: genetic analysis. Science. 1989;245:1073-80.

[15] Davidson AG, Wong LT, Kirby LT, Applegarth DA. Immunoreactive trypsin in cystic fibrosis. J Pediatr Gastroenterol Nutr. 1984;3 Suppl 1:S79-88.

[16] Sermet-Gaudelus I, Girodon E, Sands D, Stremmler N, Vavrova V, Deneuville E, et al. Clinical phenotype and genotype of children with borderline sweat test and abnormal nasal epithelial chloride transport. Am J Respir Crit Care Med.182:929-36.

[17] De Jonge HR, Ballmann M, Veeze H, Bronsveld I, Stanke F, Tummler B, et al. Ex vivo CF diagnosis by intestinal current measurements (ICM) in small aperture, circulating Ussing chambers. J Cyst Fibros. 2004;3 Suppl 2:159-63.

[18] Derichs N, Sanz J, Von Kanel T, Stolpe C, Zapf A, Tummler B, et al. Intestinal current measurement for diagnostic classification of patients with questionable cystic fibrosis: validation and reference data. Thorax.65:594-9.

[19] Cohen-Cymberknoh M, Yaakov Y, Shoseyov D, Shteyer E, Schachar E, Rivlin J, et al. Evaluation of the intestinal current measurement method as a diagnostic test for cystic fibrosis. Pediatr Pulmonol.48:229-35.

[20] Lu Y, Xiong X, Helm A, Kimani K, Bragin A, Skach WR. Co- and posttranslational translocation mechanisms direct cystic fibrosis transmembrane conductance regulator N terminus transmembrane assembly. J Biol Chem. 1998;273:568-76.

[21] Yang Y, Janich S, Cohn JA, Wilson JM. The common variant of cystic fibrosis transmembrane conductance regulator is recognized by hsp70 and degraded in a pre-Golgi nonlysosomal compartment. Proc Natl Acad Sci U S A. 1993;90:9480-4.

[22] Meacham GC, Lu Z, King S, Sorscher E, Tousson A, Cyr DM. The Hdj-2/Hsc70 chaperone pair facilitates early steps in CFTR biogenesis. EMBO J. 1999;18:1492-505.

[23] Farinha CM, Nogueira P, Mendes F, Penque D, Amaral MD. The human DnaJ homologue (Hdj)-1/heat-shock protein (Hsp) 40 co-chaperone is required for the in vivo stabilization of the cystic fibrosis transmembrane conductance regulator by Hsp70. Biochem J. 2002;366:797-806.

[24] Loo MA, Jensen TJ, Cui L, Hou Y, Chang XB, Riordan JR. Perturbation of Hsp90 interaction with nascent CFTR prevents its maturation and accelerates its degradation by the proteasome. EMBO J. 1998;17:6879-87.

[25] Pind S, Riordan JR, Williams DB. Participation of the endoplasmic reticulum chaperone calnexin (p88, IP90) in the biogenesis of the cystic fibrosis transmembrane conductance regulator. J Biol Chem. 1994;269:12784-8.

[26] Bebok Z, Mazzochi C, King SA, Hong JS, Sorscher EJ. The mechanism underlying cystic fibrosis transmembrane conductance regulator transport from the endoplasmic reticulum to the proteasome includes Sec61beta and a cytosolic, deglycosylated intermediary. J Biol Chem. 1998;273:29873-8.

[27] Cabral CM, Liu Y, Sifers RN. Dissecting glycoprotein quality control in the secretory pathway. Trends Biochem Sci. 2001;26:619-24.

[28] Vashist S, Kim W, Belden WJ, Spear ED, Barlowe C, Ng DT. Distinct retrieval and retention mechanisms are required for the quality control of endoplasmic reticulum protein folding. J Cell Biol. 2001;155:355-68.

[29] Gilbert A, Jadot M, Leontieva E, Wattiaux-De Coninck S, Wattiaux R. Delta F508 CFTR localizes in the endoplasmic reticulum-Golgi intermediate compartment in cystic fibrosis cells. Exp Cell Res. 1998;242:144-52.

[30] Bannykh SI, Bannykh GI, Fish KN, Moyer BD, Riordan JR, Balch WE. Traffic pattern of cystic fibrosis transmembrane regulator through the early exocytic pathway. Traffic. 2000;1:852-70.

[31] Prince LS, Peter K, Hatton SR, Zaliauskiene L, Cotlin LF, Clancy JP, et al. Efficient endocytosis of the cystic fibrosis transmembrane conductance regulator requires a tyrosine-based signal. J Biol Chem. 1999;274:3602-9.

[32] Weixel KM, Bradbury NA. The carboxyl terminus of the cystic fibrosis transmembrane conductance regulator binds to AP-2 clathrin adaptors. J Biol Chem. 2000;275:3655-60.

[33] Vergani P, Nairn AC, Gadsby DC. On the mechanism of MgATP-dependent gating of CFTR Cl- channels. J Gen Physiol. 2003;121:17-36.

[34] Ostedgaard LS, Baldursson O, Vermeer DW, Welsh MJ, Robertson AD. A functional R domain from cystic fibrosis transmembrane conductance regulator is predominantly unstructured in solution. Proc Natl Acad Sci U S A. 2000;97:5657-62.

[35] Randak C, Welsh MJ. An intrinsic adenylate kinase activity regulates gating of the ABC transporter CFTR. Cell. 2003;115:837-50.

[36] Stutts MJ, Canessa CM, Olsen JC, Hamrick M, Cohn JA, Rossier BC, et al. CFTR as a cAMP-dependent regulator of sodium channels. Science. 1995;269:847-50.

[37] Mall M, Boucher RC. Pathogenesis of pulmonary disease in Cystic Fibrosis. . Cystic Fibrosis in the 21st Century2006. p. 116-21.

[38] Khan TZ, Wagener JS, Bost T, Martinez J, Accurso FJ, Riches DW. Early pulmonary inflammation in infants with cystic fibrosis. Am J Respir Crit Care Med. 1995;151:1075-82.

[39] Freedman SD, Blanco PG, Zaman MM, Shea JC, Ollero M, Hopper IK, et al. Association of cystic fibrosis with abnormalities in fatty acid metabolism. N Engl J Med. 2004;350:560-9.

[40] Zaman MM, Gelrud A, Junaidi O, Regan MM, Warny M, Shea JC, et al. Interleukin 8 secretion from monocytes of subjects heterozygous for the deltaF508 cystic fibrosis transmembrane conductance regulator gene mutation is altered. Clin Diagn Lab Immunol. 2004;11:819-24.

[41] Bonfield TL, Panuska JR, Konstan MW, Hilliard KA, Hilliard JB, Ghnaim H, et al. Inflammatory cytokines in cystic fibrosis lungs. Am J Respir Crit Care Med. 1995;152:2111-8.

[42] Weber AJ, Soong G, Bryan R, Saba S, Prince A. Activation of NF-kappaB in airway epithelial cells is dependent on CFTR trafficking and Cl- channel function. Am J Physiol Lung Cell Mol Physiol. 2001;281:L71-8.

[43] Venkatakrishnan A, Stecenko AA, King G, Blackwell TR, Brigham KL, Christman JW, et al. Exaggerated activation of nuclear factor-kappaB and altered IkappaB-beta processing in cystic fibrosis bronchial epithelial cells. Am J Respir Cell Mol Biol. 2000;23:396-403.

[44] Kroncke KD. Nitrosative stress and transcription. Biol Chem. 2003;384:1365-77.

[45] BiJ Wvd, Speich R. Infectious complications after lung transplantation. European Respiratory Monograph 26: Lung Transplantation2003.

[46] Mueller C, Braag SA, Keeler A, Hodges C, Drumm M, Flotte TR. Lack of cystic fibrosis transmembrane conductance regulator in CD3+ lymphocytes leads to aberrant cytokine secretion and hyperinflammatory adaptive immune responses. Am J Respir Cell Mol Biol.44:922-9.

[47] Yoshimura K, Nakamura H, Trapnell BC, Chu CS, Dalemans W, Pavirani A, et al. Expression of the cystic fibrosis transmembrane conductance regulator gene in cells of non-epithelial origin. Nucleic Acids Res. 1991;19:5417-23.

[48] Babaev VR, Yancey PG, Ryzhov SV, Kon V, Breyer MD, Magnuson MA, et al. Conditional knockout of macrophage PPARgamma increases atherosclerosis in C57BL/6 and low-density lipoprotein receptor-deficient mice. Arterioscler Thromb Vasc Biol. 2005;25:1647-53.

[49] Bonfield TL, Thomassen MJ, Farver CF, Abraham S, Koloze MT, Zhang X, et al. Peroxisome proliferator-activated receptor-gamma regulates the expression of alveolar macrophage macrophage colony-stimulating factor. J Immunol. 2008;181:235-42.

[50] Bonfield TL, Raychaudhuri B, Malur A, Abraham S, Trapnell BC, Kavuru MS, et al. PU.1 regulation of human alveolar macrophage differentiation requires granulocyte-macrophage colony-stimulating factor. Am J Physiol Lung Cell Mol Physiol. 2003;285:L1132-6.

[51] van Heeckeren AM, Schluchter MD. Murine models of chronic Pseudomonas aeruginosa lung infection. Lab Anim. 2002;36:291-312.

[52] Bonfield TL, Hodges CA, Cotton CU, Drumm ML. Absence of the cystic fibrosis transmembrane regulator (Cftr) from myeloid-derived cells slows resolution of inflammation and infection. J Leukoc Biol.92:1111-22.

[53] Chmiel JF, Konstan MW. Inflammation and anti-inflammatory therapies for cystic fibrosis. Clin Chest Med. 2007;28:331-46.

[54] Di A, Brown ME, Deriy LV, Li C, Szeto FL, Chen Y, et al. CFTR regulates phagosome acidification in macrophages and alters bactericidal activity. Nat Cell Biol. 2006;8:933-44.

[55] Kim MJ, Cheng G, Agrawal DK. Cl- channels are expressed in human normal monocytes: a functional role in migration, adhesion and volume change. Clin Exp Immunol. 2004;138:453-9.

[56] del Fresno C, Gomez-Pina V, Lores V, Soares-Schanoski A, Fernandez-Ruiz I, Rojo B, et al. Monocytes from cystic fibrosis patients are locked in an LPS tolerance state: down-regulation of TREM-1 as putative underlying mechanism. PLoS One. 2008;3:e2667.

[57] Hubeau C, Puchelle E, Gaillard D. Distinct pattern of immune cell population in the lung of human fetuses with cystic fibrosis. J Allergy Clin Immunol. 2001;108:524-9.

[58] Armstrong DS, Grimwood K, Carzino R, Carlin JB, Olinsky A, Phelan PD. Lower respiratory infection and inflammation in infants with newly diagnosed cystic fibrosis. BMJ. 1995;310:1571-2.

[59] Brennan S, Hall GL, Horak F, Moeller A, Pitrez PM, Franzmann A, et al. Correlation of forced oscillation technique in preschool children with cystic fibrosis with pulmonary inflammation. Thorax. 2005;60:159-63.

[60] Brennan S, Sly PD, Gangell CL, Sturges N, Winfield K, Wikstrom M, et al. Alveolar macrophages and CC chemokines are increased in children with cystic fibrosis. Eur Respir J. 2009;34:655-61.

[61] Aderem A, Ulevitch RJ. Toll-like receptors in the induction of the innate immune response. Nature. 2000;406:782-7.

[62] Muir A, Soong G, Sokol S, Reddy B, Gomez MI, Van Heeckeren A, et al. Toll-like receptors in normal and cystic fibrosis airway epithelial cells. Am J Respir Cell Mol Biol. 2004;30:777-83.

[63] Bruscia EM, Zhang PX, Satoh A, Caputo C, Medzhitov R, Shenoy A, et al. Abnormal trafficking and degradation of TLR4 underlie the elevated inflammatory response in cystic fibrosis. J Immunol.186:6990-8.

[64] Wang Y, Chen T, Han C, He D, Liu H, An H, et al. Lysosome-associated small Rab GTPase Rab7b negatively regulates TLR4 signaling in macrophages by promoting lysosomal degradation of TLR4. Blood. 2007;110:962-71.

[65] Zhang Y, Li X, Grassme H, Doring G, Gulbins E. Alterations in ceramide concentration and pH determine the release of reactive oxygen species by Cftr-deficient macrophages on infection. J Immunol.184:5104-11.

[66] Andersson C, Zaman MM, Jones AB, Freedman SD. Alterations in immune response and PPAR/LXR regulation in cystic fibrosis macrophages. J Cyst Fibros. 2008;7:68-78.

[67] Painter RG, Marrero L, Lombard GA, Valentine VG, Nauseef WM, Wang G. CFTR-mediated halide transport in phagosomes of human neutrophils. J Leukoc Biol.87:933-42.

[68] Painter RG, Valentine VG, Lanson NA, Jr., Leidal K, Zhang Q, Lombard G, et al. CFTR Expression in human neutrophils and the phagolysosomal chlorination defect in cystic fibrosis. Biochemistry. 2006;45:10260-9.

[69] Deriy LV, Gomez EA, Zhang G, Beacham DW, Hopson JA, Gallan AJ, et al. Disease-causing mutations in the cystic fibrosis transmembrane conductance regulator determine the functional responses of alveolar macrophages. J Biol Chem. 2009;284:35926-38.

[70] Bae YS, Lee JH, Choi SH, Kim S, Almazan F, Witztum JL, et al. Macrophages generate reactive oxygen species in response to minimally oxidized low-density lipoprotein: toll-like receptor 4- and spleen tyrosine kinase-dependent activation of NADPH oxidase 2. Circ Res. 2009;104:210-8, 21p following 8.

[71] Zhang Y, Li X, Carpinteiro A, Gulbins E. Acid sphingomyelinase amplifies redox signaling in Pseudomonas aeruginosa-induced macrophage apoptosis. J Immunol. 2008;181:4247-54.

[72] Teichgraber V, Ulrich M, Endlich N, Riethmuller J, Wilker B, De Oliveira-Munding CC, et al. Ceramide accumulation mediates inflammation, cell death and infection susceptibility in cystic fibrosis. Nat Med. 2008;14:382-91.

[73] McDonald TV, Nghiem PT, Gardner P, Martens CL. Human lymphocytes transcribe the cystic fibrosis transmembrane conductance regulator gene and exhibit CF-defective cAMP-regulated chloride current. J Biol Chem. 1992;267:3242-8.

[74] Dong YJ, Chao AC, Kouyama K, Hsu YP, Bocian RC, Moss RB, et al. Activation of CFTR chloride current by nitric oxide in human T lymphocytes. EMBO J. 1995;14:2700-7.

[75] Moser C, Kjaergaard S, Pressler T, Kharazmi A, Koch C, Hoiby N. The immune response to chronic Pseudomonas aeruginosa lung infection in cystic fibrosis patients is predominantly of the Th2 type. APMIS. 2000;108:329-35.

[76] Tang XX, Fok KL, Chen H, Chan KS, Tsang LL, Rowlands DK, et al. Lymphocyte CFTR promotes epithelial bicarbonate secretion for bacterial killing. J Cell Physiol.227:3887-94.

[77] Casaulta C, Schoni MH, Weichel M, Crameri R, Jutel M, Daigle I, et al. IL-10 controls Aspergillus fumigatus- and Pseudomonas aeruginosa-specific T-cell response in cystic fibrosis. Pediatr Res. 2003;53:313-9.

[78] Shanshiashvili LV, Dabrundashvili N, Natsvlishvili N, Kvaratskhelia E, Zhuravliova E, Barbakadze T, et al. mGluR1 interacts with cystic fibrosis transmembrane conductance regulator and modulates the secretion of IL-10 in cystic fibrosis peripheral lymphocytes. Mol Immunol.51:310-5.

[79] Moss RB, Hsu YP, Olds L. Cytokine dysregulation in activated cystic fibrosis (CF) peripheral lymphocytes. Clin Exp Immunol. 2000;120:518-25.

[80] Tan HL, Regamey N, Brown S, Bush A, Lloyd CM, Davies JC. The Th17 pathway in cystic fibrosis lung disease. Am J Respir Crit Care Med.184:252-8.

[81] Cozens AL, Yezzi MJ, Kunzelmann K, Ohrui T, Chin L, Eng K, et al. CFTR expression and chloride secretion in polarized immortal human bronchial epithelial cells. Am J Respir Cell Mol Biol. 1994;10:38-47.

[82] Zeitlin PL, Lu L, Rhim J, Cutting G, Stetten G, Kieffer KA, et al. A cystic fibrosis bronchial epithelial cell line: immortalization by adeno-12-SV40 infection. Am J Respir Cell Mol Biol. 1991;4:313-9.

[83] Iwamura T, Katsuki T, Ide K. Establishment and characterization of a human pancreatic cancer cell line (SUIT-2) producing carcinoembryonic antigen and carbohydrate antigen 19-9. Jpn J Cancer Res. 1987;78:54-62.

[84] Schoumacher RA, Ram J, Iannuzzi MC, Bradbury NA, Wallace RW, Hon CT, et al. A cystic fibrosis pancreatic adenocarcinoma cell line. Proc Natl Acad Sci U S A. 1990;87:4012-6.

[85] Kerem E, Hirawat S, Armoni S, Yaakov Y, Shoseyov D, Cohen M, et al. Effectiveness of PTC124 treatment of cystic fibrosis caused by nonsense mutations: a prospective phase II trial. Lancet. 2008;372:719-27.

[86] Livak KJ, Schmittgen TD. Analysis of relative gene expression data using real-time quantitative PCR and the 2(-Delta Delta C(T)) Method. Methods. 2001;25:402-8.

[87] Renier M, Tamanini A, Nicolis E, Rolfini R, Imler JL, Pavirani A, et al. Use of a membrane potential-sensitive probe to assess biological expression of the cystic fibrosis transmembrane conductance regulator. Hum Gene Ther. 1995;6:1275-83.

[88] Xie J, Drumm ML, Zhao J, Ma J, Davis PB. Human epithelial cystic fibrosis transmembrane conductance regulator without exon 5 maintains partial chloride channel function in intracellular membranes. Biophys J. 1996;71:3148-56.

[89] Sorio C, Buffelli M, Angiari C, Ettorre M, Johansson J, Vezzalini M, et al. Defective CFTR expression and function are detectable in blood monocytes: development of a new blood test for cystic fibrosis. PLoS One.6:e22212.

[90] Caci E, Caputo A, Hinzpeter A, Arous N, Fanen P, Sonawane N, et al. Evidence for direct CFTR inhibition by CFTR(inh)-172 based on Arg347 mutagenesis. Biochem J. 2008;413:135-42.

[91] van Meegen MA, Terheggen-Lagro SW, van der Ent CK, Beekman JM. CFTR expression analysis in human nasal epithelial cells by flow cytometry. PLoS One.6:e27658.

[92] Sorio C, Melotti P. Editorial: The role of macrophages and their scavenger receptors in cystic fibrosis. J Leukoc Biol. 2009;86:465-8.

[93] Wilschanski M, Famini H, Strauss-Liviatan N, Rivlin J, Blau H, Bibi H, et al. Nasal potential difference measurements in patients with atypical cystic fibrosis. Eur Respir J. 2001;17:1208-15.

[94] Lange T, Jungmann P, Haberle J, Falk S, Duebbers A, Bruns R, et al. Reduced number of CFTR molecules in erythrocyte plasma membrane of cystic fibrosis patients. Mol Membr Biol. 2006;23:317-23.

[95] Schillers H. Imaging CFTR in its native environment. Pflugers Arch. 2008;456:163-77.

[96] Sterling KM, Jr., Shah S, Kim RJ, Johnston NI, Salikhova AY, Abraham EH. Cystic fibrosis transmembrane conductance regulator in human and mouse red blood cell membranes and its interaction with ecto-apyrase. J Cell Biochem. 2004;91:1174-82.

[97] Liang G, Stephenson AH, Lonigro AJ, Sprague RS. Erythrocytes of humans with cystic fibrosis fail to stimulate nitric oxide synthesis in isolated rabbit lungs. Am J Physiol Heart Circ Physiol. 2005;288:H1580-5.

[98] Dominguez C, Gartner S, Linan S, Cobos N, Moreno A. Enhanced oxidative damage in cystic fibrosis patients. Biofactors. 1998;8:149-53.

[99] Marty N, Lapchine L, Dournes JL, Agueda L, Chabanon G. Effects of five antibiotics on adhesion and haemagglutinating properties of Pseudomonas aeruginosa isolated from cystic fibrosis patients. Drugs Exp Clin Res. 1988;14:635-43.

[100] Averna M, Stifanese R, Grosso R, Pedrazzi M, De Tullio R, Salamino F, et al. Role of calpain in the regulation of CFTR (cystic fibrosis transmembrane conductance regulator) turnover. Biochem J.430:255-63.

[101] Zielenski J, Markiewicz D, Lin SP, Huang FY, Yang-Feng TL, Tsui LC. Skipping of exon 12 as a consequence of a point mutation (1898 + 5G-->T) in the cystic fibrosis transmembrane conductance regulator gene found in a consanguineous Chinese family. Clin Genet. 1995;47:125-32.